University of Nottingham Ningbo China

Department of Chemical Engineering

Molecular Simulation of CO_2 Mixtures

by

Tianhui LI

20416121

June 2023

Thesis submitted to the University of Nottingham China for the degree of MRes

Chemical Engineering and Technology

Table of contents

Acknowledgement

I want to express my sincere appreciation to Dr. Hainam Do for his diligent supervision of my project throughout the entire year. His guidance greatly enhanced my comprehension of molecular simulation and provided me with valuable research and academic writing skills.

List of Figures

List of Tables

Symbols and Abbreviations

CCS	Carbon capture and storage
VLE	Vapour–liquid equilibrium
DOS	Density of States
NS	Nested Sampling
DIA	Direct Integral Approach
GEMC	Gibbs Ensemble Monte Carlo
MD	Molecular Dynamics
MC	Monte Carlo
EOS	Equation of State
GC	Group Contribution
vdW	van der Waals
F	Helmholtz free energy
G^E	Excess free energy
$\boldsymbol{r}^N$	Position coordinates of the N particles
$\boldsymbol{p}^N$	Momentum conjugates of the N particles
A	Thermodynamic property
τ	Time interval
P	Probability
Q	Partition function
L	Length of the cubic simulation box
Ω	Density of states
h	Planck's constant
w	Weighting function
T	Temperature

p	Pressure
V	Volume
E	Energy
N	Number of molecules

Abstract

Climate change has become one of the most urgent environmental issues due to the rapid reduction of anthropogenic carbon dioxide emissions. Reducing harmful CO_2 emissions is possible through carbon capture and storage (CCS). CCS technologies rely on accurate thermodynamic property estimations of carbon dioxide mixtures with impurities to design and operate CO_2 transport processes. Consequently, researchers have begun to pay increasing attention to studies related to thermodynamic properties, particularly vapour–liquid equilibrium (VLE) of CO_2 mixtures. Conventional methods to obtain these properties, such as experiments or empirical equations of state, however, have many limitations. The phase equilibrium property can be determined using the free energy, which is the criterion for stability. However, it is extremely challenging to calculate the free energies of fluids using computer simulation. A method for obtaining the absolute Helmholtz free energy (F) was developed in this thesis. This thesis aims to use the Density of States (DOS) Partitioning Monte Carlo (MC) method to accurately and unambiguously calculate the free energy to predict the phase coexistence characteristics of binary mixtures of CO_2 with SO_2, H_2S and N_2, which are typical impurities in the captured CO_2 stream. The computed VLE from the DOS partitioning method is in good agreement with available experimental data, the equation of the state model and MC simulations. Other binary mixtures, especially those containing CO_2, can also be explored using this methodology.

Chapter 1

Introduction

1.1 Synopsis

The first part of the report gives an overview of the background of the increase in global temperature due to the heavy use of fossil fuels. And to deal with the climate crisis, since the Paris Agreement, the international community has begun to form a consensus on reducing carbon emissions and set the goal of achieving carbon neutrality as soon as possible to curb climate deterioration. Following the background, the concepts of CCS are introduced. Such technology is believed to have great potential to curb climate change, helping people to achieve the goal of carbon neutrality as much as possible without completely abandoning fossil fuels. CCS chain must be designed and operated concerning impurities present in carbon dioxide captured from energy conversion processes. To determine the level of purification needed and to evaluate the potential coexistence of impurities with CO_2, a comprehensive understanding of the thermodynamic properties of impure gas streams, especially the VLE, is essential. It has traditionally been possible to obtain these data through experiments or using empirical equations of state, but each has its limitations. The development of molecular simulation techniques, particularly molecular dynamics (MD) simulation and the Monte Carlo (MC) method, have allowed many thermodynamic properties of fluids to be computed directly. Free energy can be used to explain a wide variety of physical and chemical phenomena, but calculating free energies by molecular simulation is more challenging. Therefore, the purpose of this thesis is to address this challenge.

1.2 Background

Since the 20th century, with the explosive growth of the global population and the acceleration of the international industrial process, human beings have increasingly demanded various types of energy. Among them, fossil fuels have contributed more than 85% of the energy (Rackley, 2017), and the remaining 15% consists of nuclear, hydro and other renewable energy sources. Fossil fuels have been the main source of primary energy since the Industrial Revolution and will likely remain so for the rest of this century. **Figure 1.1** below shows the annual CO_2 emissions since 1750. The massive consumption of fossil fuels has released large amounts of CO_2 into the atmosphere and has changed the amount of carbon inherent in the atmosphere. Although human CO_2 emissions are relatively small compared to the total amount of CO_2 in the atmosphere, the rapid increase in CO_2 concentration in the short term still has a non-negligible impact on the global climate (Kilkis et al., 2020).

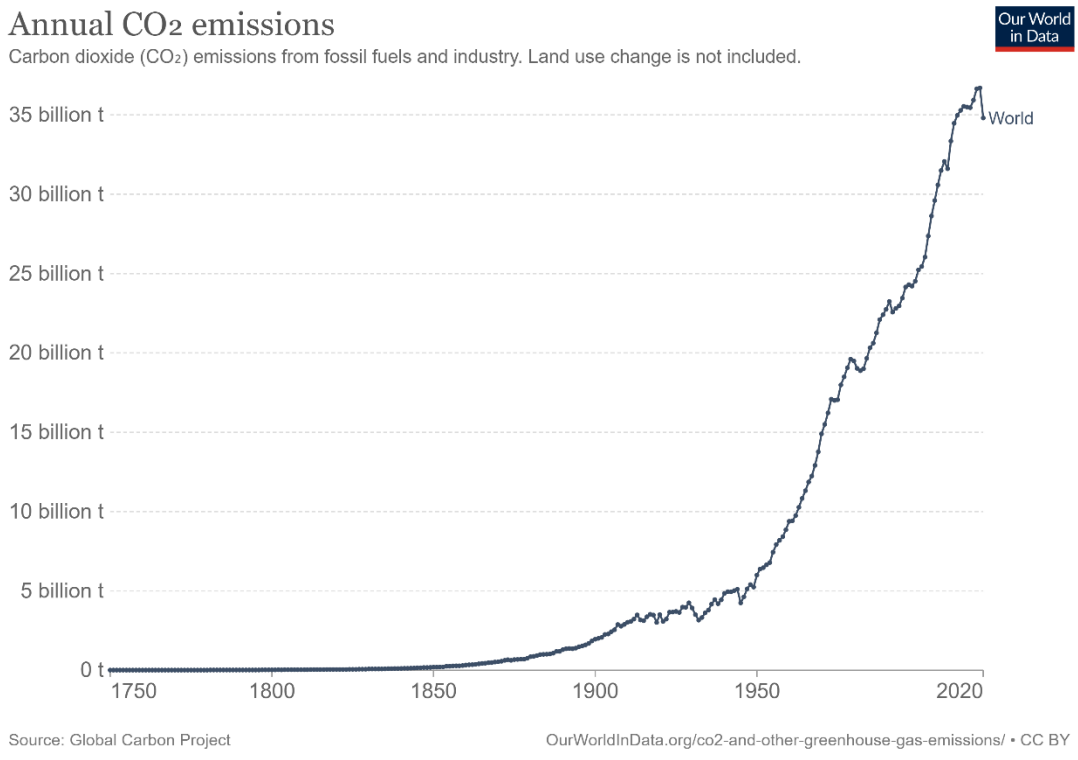

Figure 1.1. Annual CO_2 emissions since 1750 (OurWorldInData, 2020)

NASA (2022) reported that the earth's average surface temperature has risen by at least 1.1 degrees Celsius since the 1880s. As shown in **Figure 1.2**, the global average temperature since

1975 increased rapidly at a rate of 0.15-0.2 degrees Celsius per decade. Global warming is not only an environmental issue. Still, it has also caused serious threats in important fields such as the global economy, energy security and food security, etc., which is an unprecedented challenge to human beings. Since the millennium, a series of problems caused by global warming has gradually attracted the international community's attention. The deficiencies in the previous economic development model have become imminent, and the establishment of a low-carbon, sustainable development model has gradually become the consensus of various governments (Li et al., 2022).

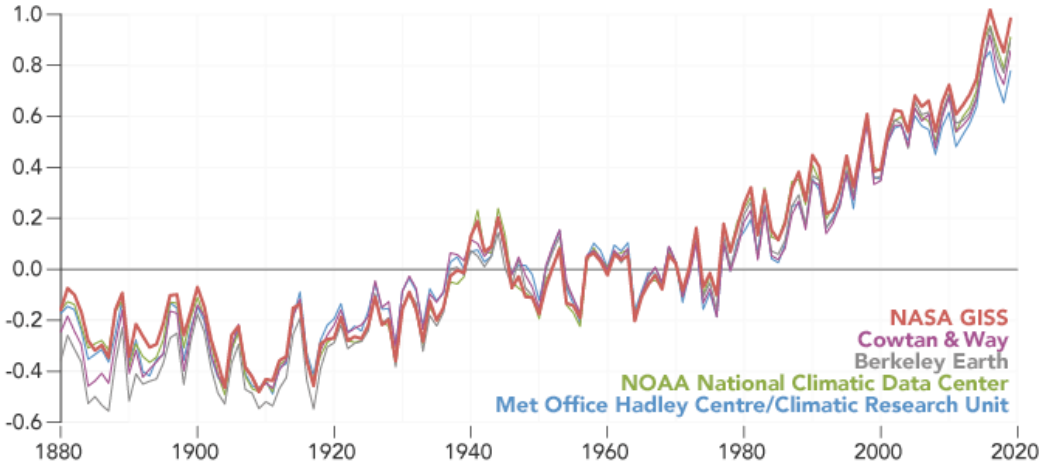

Figure 1.2. Global temperature records by the different research groups (NASA, 2022)

In December 2015, official representatives from 196 countries and regions gathered in Paris to adopt the landmark Paris Agreement (PA). This agreement is a legally binding international climate treaty that aims to bring every country into the same great cause and make a corresponding effort on climate change. The 196 governments that signed the pact pledged to work together to keep the world's average temperature no more than 2 °C above pre-industrial levels, ideally lower than 1.5 °C (United Nations, 2015). In 2018, the Intergovernmental Panel on Climate Change (IPCC) assessed the impact of a 1.5°C rise in global temperature compared to pre-industrial levels and suggested the need and urgency to delay global warming. The report of IPCC (2018) detailed that containing the climate rise within 1.5 degrees Celsius will largely reduce the frequency of natural disasters (e.g., floods, droughts, etc.) from the perspective of short-term and long-term impacts, respectively. Curbing climate rise will also greatly reduce

risks to human survival due to rising sea levels and reduced biodiversity (Zhao et al., 2022). Therefore, cutting down the emissions of greenhouse gases and mitigating global warming have become the goal of all humanity.

In addition to determining the overall goal of advocating a green economy and slowing global warming, the PA specifies a series of active measures regarding environmental protection and human survival. These include achieving global climate neutrality by the mid-21st century (around 2050). In order to realize this grand vision, every country needs to reach peak carbon emissions as early as possible. Also, as the member states of the PA, all countries are required to set greenhouse gas (GHG) emission reduction targets that suit their national conditions and submit climate action plans every five years, known as nationally determined contributions (NDCs). As the 23rd country to ratify the Paris Agreement, China became a PA member state in 2016 and submitted its own NDC in 2020. In addition to China's practical actions in the field of carbon emissions, more and more other countries are also actively responding to the carbon neutrality initiative and take corresponding steps. At the One Earth Summit in 2017, 32 countries worldwide signed up for the Carbon Neutrality Coalition (CNC) to achieve carbon neutrality goals. In 2019, 66 countries and regions pledged to achieve zero carbon emissions and established the Alliance for Climate Ambition at the UN Climate Action Summit (UNFCCC, 2019).

As the world's second-largest economy after the USA, China has become the world's factory in recent years. China produces the world's largest amount of steel, cement, and other building materials and also manufactures the world's largest number of industrial supplies such as ships, machine tools and automobiles. Among them, fossil energy plays an irreplaceable and important role in the process of China's industrial rise (Admos, 2019). However, the rapid economic development has also produced corresponding environmental costs, and the excessive consumption of fossil fuels has led to the persistently high carbon emission level in China. Since 2011, China has become the world's largest emitter of CO_2 as shown in the **Figure 1.3**.

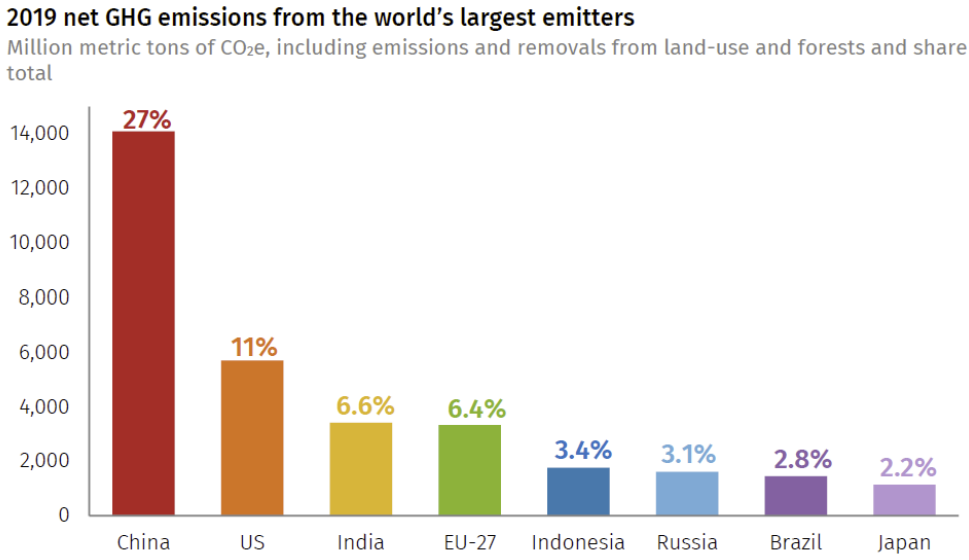

Figure 1.3. China becomes the world's largest emitter of CO_2 (Kate, et al., 2021).

As mentioned above, environmental protection and sustainable development have become the consensus of today's international community. Therefore, as the largest carbon emitter, China faces enormous pressure to reduce CO_2 emissions (Lin and Xu, 2020). Under this circumstance, China has taken the initiative to assume its international responsibilities as the most populous country in the world, formulated many policies to control carbon emissions, and made efforts to promote and develop a green and sustainable economy. For example, in 2020, Chinese President Xi Jinping made a declaration at the United Nations that China would peak its carbon emissions by 2030 and achieve carbon neutrality by 2060 (shown in **Figure 1.4** below). China has demonstrated its support for the PA to the international community with practical actions, leading the world to move towards the goal set on the PA (global average temperature increase of no more than 1.5 °C), which reflects its determination to develop a green economy.

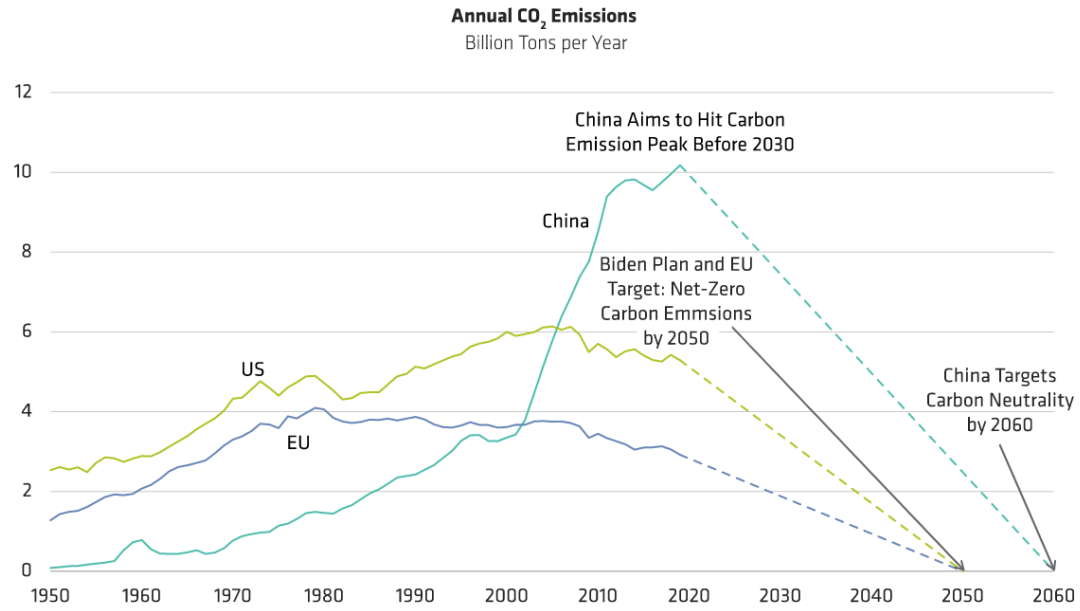

Figure 1.4. China's 2060 carbon neutrality plan (Lin and Zeng, 2021).

As introduced above, China plans to achieve the goal of peaking carbon emissions by 2030. The term carbon peak mentioned here refers to a year in which the CO_2 emissions of an industry or region reach their high historical values (peak). After getting the peak, the carbon emissions of this industry or region will transition to a relatively stable stage and begin to decline after a period, which means that economic growth becomes no longer positively correlated with CO_2 emissions. It is one of the important indicators of achieving the goal of a green economy. Another term, 'carbon neutrality' means that the CO_2 emissions produced by social production and life are equal to the fixed CO_2 emissions absorbed by various biological and chemical means. To achieve the goal of carbon neutrality, companies and individuals need to replace traditional fossil fuels with clean energy as much as possible while avoiding waste of energy and resources. However, carbon neutrality is an aspirational goal; for certain industries, net CO_2 emissions are unlikely to be zero. For example, even if all electricity is powered by clean energy (tidal, solar, wind and hydro), traditional industries such as steel and coal production will still have carbon emissions. Therefore, establishing a carbon sink or carbon budget system is required to make it close to neutrality (Becker et al., 2020).

The above section explains what carbon neutrality means for a country or region; however, on a global scale, carbon neutrality is a much more ambitious goal. The PA proposes that in the future, efforts need to be made to keep the global average temperature below 1.5 °C of the pre-industrial average. This means that in a limited period, the net emission of greenhouse gases into the atmosphere must be close to zero. In other words, carbon neutrality can be achieved when the greenhouse gases absorbed by various human activities can offset the greenhouse gases that people produce. By monitoring the carbon emissions from the industry in 2021, Liu et al. (2022) assessed the progress in achieving the goal of carbon neutrality and estimated the remaining carbon budget. The dark blue line in **Figure 1.5** illustrates the predicted CO_2 emission mitigation pathway if the PA needs to be reached by 2050. Also, in this report, Liu et al. concluded that if the trend in 2021 continues, the carbon budget may be consumed half a year ahead of schedule with a 67% probability (Liu et al., 2022).

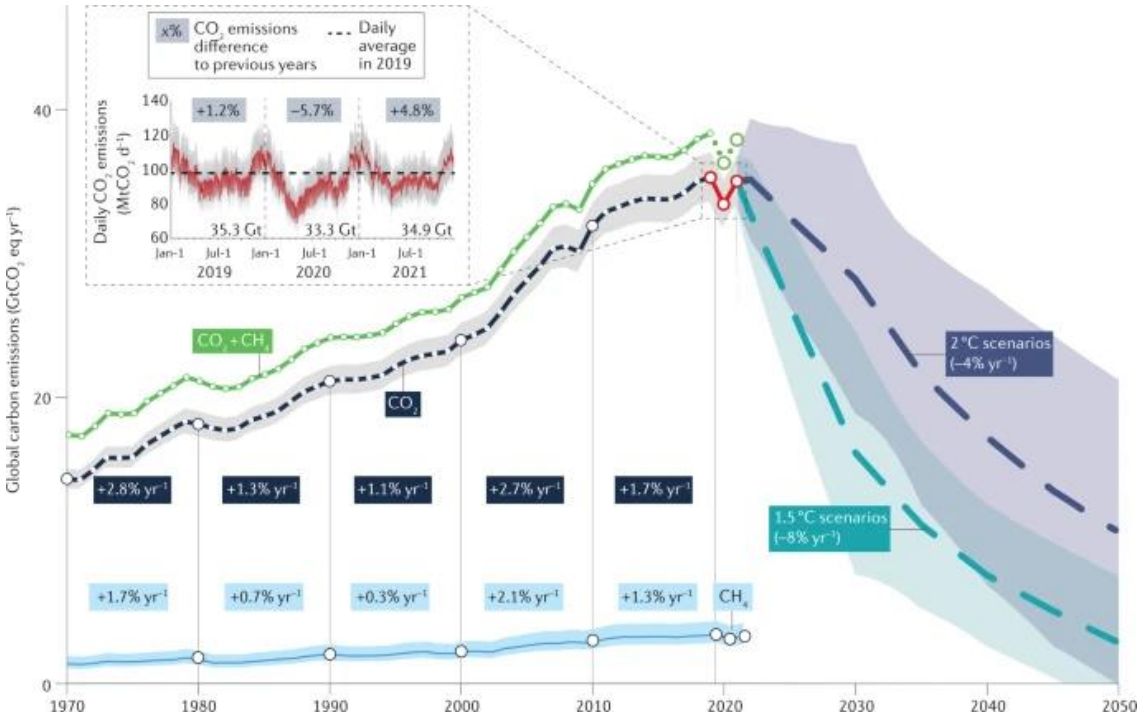

Figure 1.5. Predicted CO_2 emission mitigation pathways (dark blue) to achieve carbon neutrality in ten years (Liu, et al., 2022)

Of course, the greenhouse gas is not only CO_2, but because of its extremely high amount, CO_2 is the main component of greenhouse gas and seriously affects the climate. According to the researchers' calculations (Su, 2021), the cumulative global CO_2 emissions reached a staggering

2,500 Gt in 2019, four times more than in 1950. Therefore, CO_2 is usually the main objective of the international community to achieve zero greenhouse gas emissions. Currently, the four terms used to represent the goal of curbing global temperature rise proposed by PA are carbon neutrality, net-zero carbon emissions, climate neutrality, and net-zero emissions, respectively.

The four terms mentioned above have very similar names, but they all have their meanings in a strict sense. The IPCC's 2018 report defines the alignment of the concepts of carbon neutrality and net zero carbon emissions. Carbon neutrality can be reached when the CO_2 emissions produced by social production and life equal the CO_2 absorption. Thus, the object described by the terms carbon neutrality and net-zero carbon emissions is mainly CO_2. Net-zero emissions generally refer to the balance between the production and absorption of greenhouse gases, including CO_2, and other gases, such as methane. Therefore, if net-zero emissions are used as the test metric, the degree to which the target is achieved depends on the gas of interest. For example, if a chemical plant targets zero methane emissions, engineers only need to focus on how much methane the plant absorbs or releases each year, not CO_2. Different from the above three concepts, climate neutrality is not specifically limited to one or certain greenhouse gas. Climate neutrality refers to the macro impact of human activities on climate, as greenhouse gas emissions are only part of the cause of climate change. Other human activities such as clearing land, clearing forests, and building infrastructures such as roads and dams can also profoundly impact the climate. It is worth noting that the carbon neutrality and net zero greenhouse gas emissions mentioned above are not necessary conditions for climate neutrality; in other words, as long as the local climate conditions are not affected, both methane and CO_2 emissions are acceptable.

These concepts are dull and confusing to some extent, so even though the IPCC has clearly defined these concepts and explained their differences in the report, there are still deviations in understanding these definitions among policies in many countries. In many countries (such as France, Finland, Japan, etc.), climate neutrality is still a strategic goal of economic development; however, at the policy level, most policies and laws revolve around net zero carbon emissions.

1.3 CO_2 Capture and Storage (CCS)

As mentioned in the section, greenhouse gas emissions from human activities are dramatically affecting the global climate. Among these greenhouse gases, CO_2 is thought to be mainly responsible for the increase in global surface temperature (Li et al., 2011). For the goal of a green economy, humanity has begun to study how to reduce the existing CO_2 in the atmosphere, and CCS technologies have emerged as the times require. The IPCC recognizes CCS as one of the technologies that can effectively reduce mid-term CO_2 emissions in the atmosphere (Mantovani, 2012). This technology usually refers to utilizing physical or chemical technics to separate the carbon from the combustion of fossil fuels before being directly released into the atmosphere. Then the CO_2 can be transported to a storage site and permanently stored (Metz et al., 2005).

Currently, most research on CCS is devoted to the application of CCS in power plants and the storage of captured CO_2 in geological reservoirs because power plants are the largest carbon emission stationary sources in the world, accounting for 80% (Matteo et al., 2013). The remaining 20% comes from other industrial sectors, such as steel plants (5%), cement plants (7%) and oil refineries (6%). The IPCC also proposes that if CCS is widely used in the power generation industry, CO_2 emissions per kWh of electricity can be reduced by up to 90%. Therefore, the promotion of CCS can accelerate the realization of the vision of a green economy as an effective complement to the clean energy strategy (Li et al., 2011).

Today, fossil fuels remain the dominant energy source for much of the world, and many countries worldwide are making efforts to expand the share of clean energy in the energy mix. Various policies have been formulated for this purpose. For example, increasing investment in photovoltaics, hydropower generation, or tax exemptions on goods produced using clean energy to encourage companies to use. But inevitably, since fossil fuels have been deeply bound to industrial civilization, people cannot get rid of their dependence on fossil fuels in a short time. Therefore, CCS may have enormous potential to play a significant role in addressing climate change for the remainder of this century. From this perspective, the basic role of CCS can be viewed as the transition to full use of clean energy, allowing people to continue to use

fossil fuels while reducing carbon emissions, thereby delaying global warming. However, there are currently only four large CCS commercial projects worldwide, each capturing and fixing roughly 1 Mt of CO_2 annually. If CCS truly serves as a solution to curbing climate change, this number must reach the level of Gt (Herzog, 2011).

CCS has not been promoted and used on a larger scale because its cost has remained high. In summary, there are mainly three steps in a CCS system, as shown in **Figure 1.6**: capture (or separation), transportation and injection.

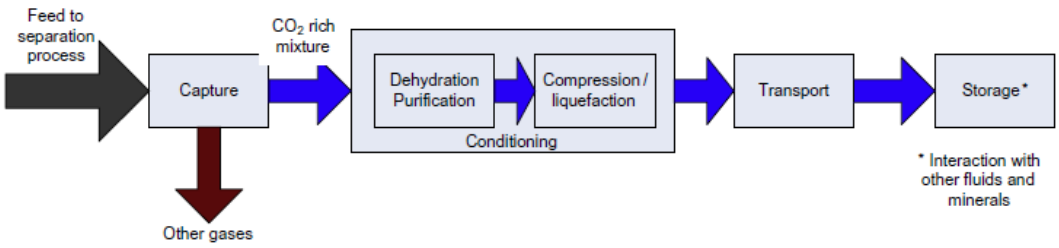

Figure 1.6. Main steps of the CCS chain (Li H, et, al., 2011).

The latter two steps, transportation and storage, are inexpensive because the existing technology is quite mature. The real reason that makes CCS expensive is the separation, which accounts for two-thirds of the entire system cost, hindering the large-scale commercialization of CCS. Engineers and scientists have made many attempts and efforts to make the process of separating CO_2 efficient and cost-effective. Based on the chemical reaction process during the combustion of fossil fuels, three carbon capture techniques have been proposed: pre-combustion capture, oxy-fuel combustion, and post-combustion capture, respectively (Li et al., 2011).

As illustrated in **Figure 1.7**, pre-combustion capture refers to the pre-reaction of fuel with air to produce a mixture rich in H_2 and CO (also known as syngas), which is then passed through a catalyst to convert the CO into CO_2. Finally, the separation of hydrogen and CO_2 can be easily achieved in several ways. The obvious disadvantage of this approach is the requirement for gas turbines that can operate efficiently in H_2-rich conditions.

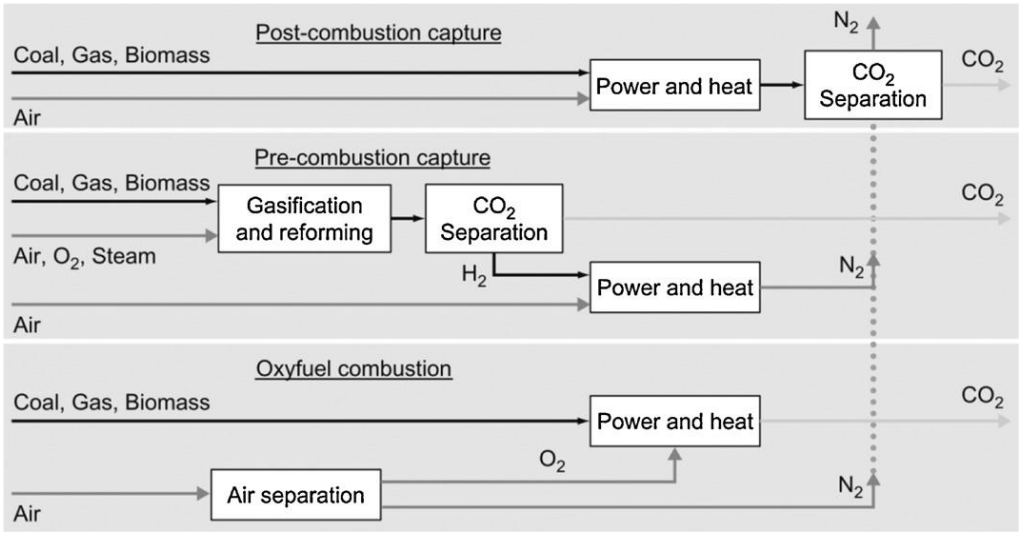

Figure 1.7. Three proposed methods for CO_2 separation (Li, et al., 2011).

Oxyfuel combustion allows the fuel to carry out the combustion reaction in a pure environment with only oxygen so that the product is only CO_2, which can be directly transported and stored. The need for pure oxygen makes this method expensive and unfavourable for commercial deployment. The purpose of post-combustion capture is to remove CO_2 from the emissions produced after the combustion of the fuel, which usually consists of N_2 and CO_2. This method is currently the most feasible because some of the technologies involved can be implemented directly by retrofitting the flue without replacing the power system.

1.4 Conventional Method

Impurities are always unavoidable in the process of capturing CO_2 through energy conversion. According to the previous study (Li H et al., 2009), the development and implementation of CCS systems are significantly affected by impurities. Li H et al. (2011) have revealed it is critical to accurately assess the thermodynamic properties of CO_2 mixtures, especially VLE, when designing the procedure of CO_2 gathering and undesirable gas separating to enhance the efficiency of the whole sub-processes involved in both capture and transport systems. Both the fuel used and the technology used in the capture process determine the type and number of impurities existing in CO_2. For example, H_2O is the dominant impurity in the CO_2 stream captured after the combustion of amine solution, hence the fuel is relatively clean.

Nevertheless, it is predicted that burning oxy-fuel can create a comparatively higher concentration of unwanted substances in the gathered CO_2 stream, and the production of more intricate composition happens and exist in the gathered CO_2 stream when Integrated Gasification Combined Cycles are employed. Previous studies (IPCC, 2005; Li H, 2008; Visser, 2008) have summarized the possible impurities produced by various oil industries and the processes of fuel conversion in **Table 1.1**. Meanwhile, **Table 1.2** shows the probable ranges of the impurity concentration in the streams obtained from the CO_2 gathering process (Li et al., 2011).

Table 1.1. Possible impurities (IPCC, 2005, cited in Li H, et al.,2011)

Description	**Possible Impurities**
CO_2 captured from natural gas sweetening	CH_4, amines, H_2O
CO_2 captured from heavy oil production and upgrading	H_2S, N_2, O_2, CO, H_2O, H_2, COS, Ar, SO_X, NO_X
CO_2 captured from power plants using post-combustion capture	N_2, amines, H_2O, O_2, NH_3, SO_X, NO_X
CO_2 captured from power plants using oxy-combustion capture	N_2, O_2, SO_2, H_2S, Ar
CO_2 captured from power plants using pre-combustion capture	H_2, CO, N_2, H_2S, CH_4

Table 1.2. Impurity concentrations (Li H, 2008 and Visser, 2008 cited in Li H, et al.,2011)

Component	**Min mol%**	**Max mol%**
CO_2	75	99
N_2	0.02	10
O_2	0.04	5
Ar	0.005	3.5
SO_2	< 0.0001	1.5
H_2S+COS	0.01	1.5
NO_X	0.0002	0.3
CO	0.0001	0.2
H_2	0.06	4
CH_4	0.7	4

Several experimental and theoretical methods for obtaining the VLE of the working fluid are proposed. The experimental design and implementation are often based on phase equilibrium data of mixtures containing CO_2 to provide the basis, which needs to analyse the thermodynamic characteristics of the mixture containing CO_2 when each phase reaches equilibrium. Essentially, the thermodynamic parameters such as component concentration, specific volume, and entropy of the mix at phase equilibrium can be figured out by analysing the thermodynamic attributes of CO_2-containing combinations when the phases are in balance and by determining the thermodynamic parameters (e.g., temperature, pressure, etc.) at equilibrium. So is to provide a basis for the analysis of the thermodynamic parameters related to the CCS, the selection of the separation method, the separation purity, the separation rate, the separation energy consumption and the design of the system process and equipment.

1.4.1 Experiment

The experimental method is the most straightforward and reliable way for the phase equilibrium data acquisition; that is, a series of properties such as density and composition of each phase state under the condition of phase equilibrium are measured at a given pressure and temperature, and then the relationship between temperature, pressure, and molar composition of each phase at equilibrium is calculated by the method of computational correlation. In the recent century, more researchers have focused on investigating the VLE properties of CO_2 mixtures and carried out numerous experiments. Experimental methods can be divided into analytical and non-analytical methods in terms of whether samples are taken for analysis. The analytical way the experimental determination is carried out by direct sampling gives relatively accurate results under normal circumstances; however, the error is greater for special systems, such as determining the thermodynamic properties of infinite dilutions. The analytical method can be divided into static methods and dynamic methods according to how the system is brought to equilibrium during the experimental determination. In addition, Valtz et al. (2002), have developed some experimental systems that are highly accurate in estimating vapour-liquid equilibrium via static methods. Dynamic methods are further divided into recirculation methods and continuous flow methods. For instance, many investigators have also measured the VLE

using recirculation methods, which can expedite the system equilibrium compared to static methods. An apparatus utilising the vapour-phase single-recirculation method was designed by Bobbo et al. (1998), and the system was improved by Zhao (2017) and Dong (2018), and Meng et al. (2018). Moreover, another apparatus was developed by Lim et al. (2002) based on the vapour-liquid double-recirculation method (Nie et al., 2018). The non-analytical process does not require direct sampling but employs an indirect approach to determine properties such as component content at phase equilibrium. This method uses the solution's dew point, bubble point, volume change and chromatographic slope to assess phase equilibrium (Yang, 2016). By evaluating hundreds of working fluids with the assistance of researchers, it was possible to determine the VLE of these fluids.

1.4.2 Theoretical Research

There are two major methods widely employed in theoretical studies that are the equation of state (EOS) and the group contribution (GC) (Li H et al., 2011). EOS relates the value of a given substance's pressure, volume, and temperature into a mathematical equation. Essentially, the deviation functions of ideal gas dynamic condition and phase equilibrium can be obtained based on the relationships inside gas provided by typical thermodynamics. According to this, even though the mixture component data is limited, commonly only including temperatures at a critical level, acentric factors, and pressures, the thermodynamic properties in the case of vapour and liquid phases can also be determined. A large scale of temperatures and pressures involving two different zones that are sub-critical and supercritical can employ the equation of state for mathematical analysis. The equations of state have been divided into various categories based on previous research, such as cubic equations from the van der Waals family and extended virial equations family. Performances of different models have been proved to be varied depending on various attributes, components, and states (Abbott, 1979; Danesh, 1991; Yang, 2003). The most common EOS associated with CCS, especially those estimated in previous papers, are discussed as follows.

The cubic equations can be considered the simplest EOS, which makes them a favorite choice while dealing with the applicable engineer. As a critical point can be forecasted, the condition

of VLE can also be quantitatively obtained with this equation. Van der Waals raised the EOS in 1873; after that, scientists devoted themselves to improving the cubic equation by introducing two or more parameters to predict the equilibria attributes of volumetric fluid and phase accurately. Hence, there were more and more cubic equations proposed since 1873, for instance, the Redlich–Kwong EOS (RK) by Kwong and Redlich (1949), Soave–Redlich–Kwong EOS (SRK) by Soave (1972), the Peng–Robinson EOS (PR) by Peng and Robinson (1976) and so on. Cubic EOS has commonly been deemed an outstanding model tool for phase equilibrium (Li et al., 2011).

In terms of the modelling ability in VLE of those RK, PR, and SRK cubic equations of state, also involving the Perturbed-Chain SAFT (PC-SAFT) and Statistical Associating Fluid Theory (SAFT), Diamantonis et al. (2013) utilizing different binary VLE mixed with CO_2, including SO_2, H_2S, CH_4, O_2, and N_2, as well as the mixture fluids of CO_2−N_2−O_2.

EOS has its advantages over other modelling approaches, and the fact that multiple thermophysical properties can be calculated using relatively simple calculations with EOS is undoubtedly its most endearing advantage. Moreover, several EOSs allow researchers to employ the most adaptable one. Then, the accurate evaluation with EOS is capable of fully satisfying the demand of engineering work. EOS also own some disadvantages, such as finite applications. The reason is some of the property constants of the equation are calculated utilizing the traditional working fluids in a general way, and several parameters, especially for the coefficients of interaction, are absent. Those coefficients can only be determined from previous experience, which is a tedious workload. But these shortcomings are relatively addressed by the GC method, which is based on a hypothesis that thermophysical characteristics for targeting fluids are the function of those parameters which are reliable to molecular structure in fluids. GC means assumes that every single component consists of different functional groups based on its molecular structure, and each group is capable of contributing to thermophysical characteristics, which corresponding parameters of other groups can present. VLE data from previous experiments help to determine parameters of functional groups, commonly those traditional working fluids with known molecular structures. Besides, several novel working fluids can be designed based on this functional group hypothesis.

However, GC also has limitations. It is hard for this method to handle isomer systems since it is derived from some specific approach. An example condition is that the existence of molecules with a novel functional group that is not included in the database of group contribution method would make difficulties in the properties evaluation of working fluids (Nie et al., 2018).

Besides, inter-component interactions are explored by correspondingly establishing hundreds of mixing rules to predict the VLE of work fluids mixture with the help of cubic equation of state (EOS). Research on mixing rules has received a lot of scholarly attention in recent years, and there are only two dominant types, van der Waals (vdW) mixing rules and excess free energy (G^E) mixing rules (Kwak and Mansoori, 1986; Tochigi et al., 1995, cited in Wu, et al., 2022). The combination of using the cubic EOSs and van der Waals mixing rules is commonly used in VLE since this combination is simple and relatively accurate (Wu et al., 2022). The PR EOSs using vdW mixing rules with a novel model, which are closely associated with acentric factors and fluorine atomic numbers, were put forward by Chen et al. in 2008 to finish the prediction of VLE properties within the context of HFC/HC binary mixtures. For the purpose of predicting the phase characteristics of binary systems consisting of ethane + n-alkane and methane + n-alkane, Duaret et al. (2014) proposed an exponential function, known as the kij model, that establishes a relationship between the critical temperature and temperature by utilizing the PR and RKPR EOS as supportive components (Wu et al., 2022). Besides, a PR-VDW model based on the temperature-reliable kij was developed by Zhang et al., and the prediction covered kij for a total of 351 binary systems was achieved using an experimental database (Nie et al., 2018). With respect to the excess free energy (G^E) mixing rules, they are appropriate for behavior prediction of liquids in the case of greatly non-ideal systems. The studies involve several mixing rules for the EOS/GE model, for example, HV, WS, MHV1, and MHV2 et al. (Nie et al., 2018).

Excess Gibbs free energy visualizes energy behaviors into specific parameters in the model employing Cubic EOSs. It is proved by Qin et al. that the VLE data was highly accurate while employing the o PR-WS-MUNIFAC model to evaluate not only the binary mixture of R152a + R1234yf but also the ternary mixture of R32 + R125 + R134a (Qin et al., 2018).

Su et al. (2017). evaluated and summarized capabilities and limitations in the prediction of several prevalent cubic EOSs and mixing rules like VDW and Excess free energy employed in VLE calculations of working fluids, especially focusing on how the interaction coefficients impact predictions under various mixing modes and how to determine this parameter. Due to the high dependence of the interaction coefficients on empirical data, a perfect model for predicting that can provide a better prediction for the large range of mixtures has not been proposed yet. In summary, determining interaction coefficients for binary systems has apparent drawbacks (Nie et al., 2018).

It is clear from the above pieces of literature that both experimental and theoretical approaches have their specific limitations. For instance, obtaining data for both traditional and novel working fluids from the experiment is persuasive but costly and time-consuming. Therefore, experiments are not considered the initial choice and primary assessment while dealing with many working fluids and mixtures. Apart from that, it is experiments data providing the basis of parametrization of theoretical methods like EOSs and GCs mentioned above. Therefore, the absence of experimental results would lead to failure in accurate VLE prediction of novel working fluids using those models. In addition, some research by Lasala (2016, 2017) has pointed out that the optimization of models, in theory, requires the uncertainty of data from experiments. Parameterization of thermodynamic models can be limited by the uncertainty in experiments in every measurement result, which is a general issue affecting this process (Nie et al., 2018).

1.5 Molecular Simulation

Temperature, density, volume, heat capacity, and other macroscopic properties are determined by specific interactions between molecules on the microscopic scale. The research for connections between the microscopic and macroscopic worlds has been a popular study, and adequately explaining this connection is essential for determining fluids' thermodynamics and transport properties. Molecule simulations have made great progress, which can also provide information about their structure and dynamics. Calculations obtained by molecular computer simulations can be performed to arbitrary accuracy if the simulation time is long enough. Unlike

complex experimental processes, molecular simulations are reliable tools for studying the phase equilibrium of fluids from a microscopic point of view, without the constraints of experimental conditions, equipment failures and safety hazards caused by high pressures, etc. It has the advantages of safety, speed and accuracy and can be extended to research areas where experimental data are insufficient (Yang, 2016).

The development of molecular simulation, which includes MD simulation and the MC method, has made significant advances in recent years. The molecular simulation method is a method to link macroscopic phenomena to molecular interactions; this technique is highly predictive and efficient for computation because it is based on statistics. In particular, Li et al. (2011) have demonstrated that molecular simulation is a versatile and important method for studying CCS since it overcomes the limitations of inadequate experimental data within traditional approaches. Having determined the molecular structure of the fluid in which the work is, the VLE can be predicted using molecular simulation. The Boltzmann distribution can be used to determine some configurations of the particle system in the Monte Carlo method. Through sampling in these configurations, one can calculate the thermodynamic properties of the system using the ensemble average (Frenkel and Smit, 2002). While MC can calculate VLE efficiently (Ramdin et al., 2016), the results are not that accurate regarding dynamic data (Theodorou, 2010). Molecular dynamics simulation is based on the solution of Newton's second law for particle systems to determine the momentum and position at each time step of a particle. Thus, this can provide a more accurate portrayal of the actual particle movement. As well as processes that are in equilibrium, for instance, VLE, MD can also be used to determine non-equilibrium processes (Li et al., 2010) and reactions (Huo et al., 2017). Following will be a discussion of the details of MC and MD.

1.5.1 Statistical Thermodynamics

As a result of molecular simulation, all thermophysical properties can be predicted within a theoretical framework, namely statistical thermodynamics (McQuarrie, 1976; Rowley, 1994). In statistical thermodynamics, also known as equilibrium statistical mechanics, a connection exists between the macroscopic and microscopic worlds. It uses total energy to obtain

thermodynamic properties, which are determined by a particle's position and momentum. It is a process of integrating over the momenta and positions of the molecules contained in the system. When a system is observed at a particular time, its state depends entirely on the 3N position coordinates (x, y, z) $\boldsymbol{r}^N(t)$ and 3N momentum conjugates $\boldsymbol{p}^N(t)$ of the N particles, identifying a phase point in 6N dynamical coordinates. Statistical mechanics is the theory that explains macroscopic physical properties A by applying the microcosmic instantaneous replica $A[\boldsymbol{p}^N(t), \boldsymbol{r}^N(t)]$ to the time average A, utilizing the following equation to calculate the time average A_{ave}.

$$A_{ave} = \lim_{\tau\to\infty} \frac{1}{\tau} \int_0^\tau A[\boldsymbol{p}^N(t), \boldsymbol{r}^N(t)]dt \qquad (1.1)$$

in which t represents the time and τ represents the time interval. By integrating Newton's equations of motion, the integral value calculated in Equation 1.1 approaches the property's actual value as the measured time increases to infinity. Such calculations are performed using molecular dynamics simulation. As seen from the equation above, if the system's initial state is known, it can be integrated to obtain the time average A_{ave}. However, due to the huge number of particles in the macroscopic system (10^{23} orders of magnitude) and the infinite number of corresponding microscopic states, A_{ave} is extremely complex. The system's initial state cannot even be determined, let alone Newton's equations of motion, and the movement of particles can be calculated.

Gibbs (1902) introduced the concept of an ensemble 1902: an ensemble is a set of systems with a fixed number of molecules *N* utilized in statistical mechanics. The averages derived from these ensembles are frequently referred to as ensemble averages. Molecular simulation is based on ensemble theory. The ensemble theory, which aims to derive thermodynamic properties A from a molecular perspective, aims to determine how likely a set of molecules will be in a particular energy state (Nie et al., 2018). The time average can then be replaced by the ensemble average $\langle A \rangle$:

$$\langle A \rangle = \iint A(\boldsymbol{p}^N, \boldsymbol{r}^N) P(\boldsymbol{p}^N, \boldsymbol{r}^N) d\boldsymbol{p}^N d\boldsymbol{r}^N \qquad (1.2)$$

where $P(\boldsymbol{p}^N, \boldsymbol{r}^N)$ is the probability that a configuration with momenta $\boldsymbol{p}^N$ and positions $\boldsymbol{r}^N$ will be found. As known from Equation 1.2, the result of the integration of the system in all possible configurations $(\boldsymbol{p}^N, \boldsymbol{r}^N)$ is what provides the solution. MC simulations can be used to compute the ensemble average $\langle A \rangle$, which samples in accordance with a probability density $P(\boldsymbol{p}^N, \boldsymbol{r}^N)$ based on a set of fixed macroscopic conditions (such as NVT, NpT, etc.).

Molecular mechanics simulations of fluids were first achieved by Metropolis et al. (1953), when a scheme was developed to obtain the ensemble averages using sampling obeyed the Boltzmann distributions. This resulted in MC simulations. Following this, Alder (1957) realized that it was feasible to simulate the behavior of real systems by utilizing periodic boundary conditions and it was based on the integration of equations of motion involving only a small number of particles. This was the first molecular dynamics simulation of a real system. A fundamental principle of statistical mechanics is the ergodic hypothesis, which states that at thermodynamic equilibrium, the time average A_{ave} is the same as ensemble average $\langle A \rangle$.

However, there are some differences between the MC and MD, and the **Figure 1.8** depicts the flow chart for both methods. The MC simulation is stochastic and does not include information regarding particle momentum or other time-dependent characteristics. Alternatively, MD is deterministic and keeps track of both point positions and momenta as well as calculates forces and accelerations. In contrast to MD, MC does not involve the use of time, and therefore it cannot be used to calculate properties such as diffusion coefficients, viscosity or thermal conductivity. MC simulations do not take into account the order in which configurations are generated. The configurations in MD simulations, however, are determined by initial conditions and occur in order of time, so there is limited capacity to improve their sampling efficiency other than adjusting the time step or using special non-Cartesian coordinates. Due to this, MC is a more efficient sampling method in phase space than MD. Additionally, MD is typically capable of advancing velocity and position, which facilitates the exploration of local phase spaces. MC is capable of exploring a relatively large area, even a distinct region of phase space. In contrast, when calculations are performed on VLE, the focus is only on the configuration of equilibrium that is stable. The process by which this configuration is reached is not of significance (Nie et al., 2018). Thus, MC is a widely used method for the determination of the

VLE. The determination of vapour-liquid coexistence characteristics can be achieved through various MC methodologies, including the NPT plus test particle approach, Gibbs-ensemble method, and grand canonical with histogram reweighting. However, the accurate estimation of solid-fluid and solid-solid coexistences continues to pose difficulties within molecular simulations.

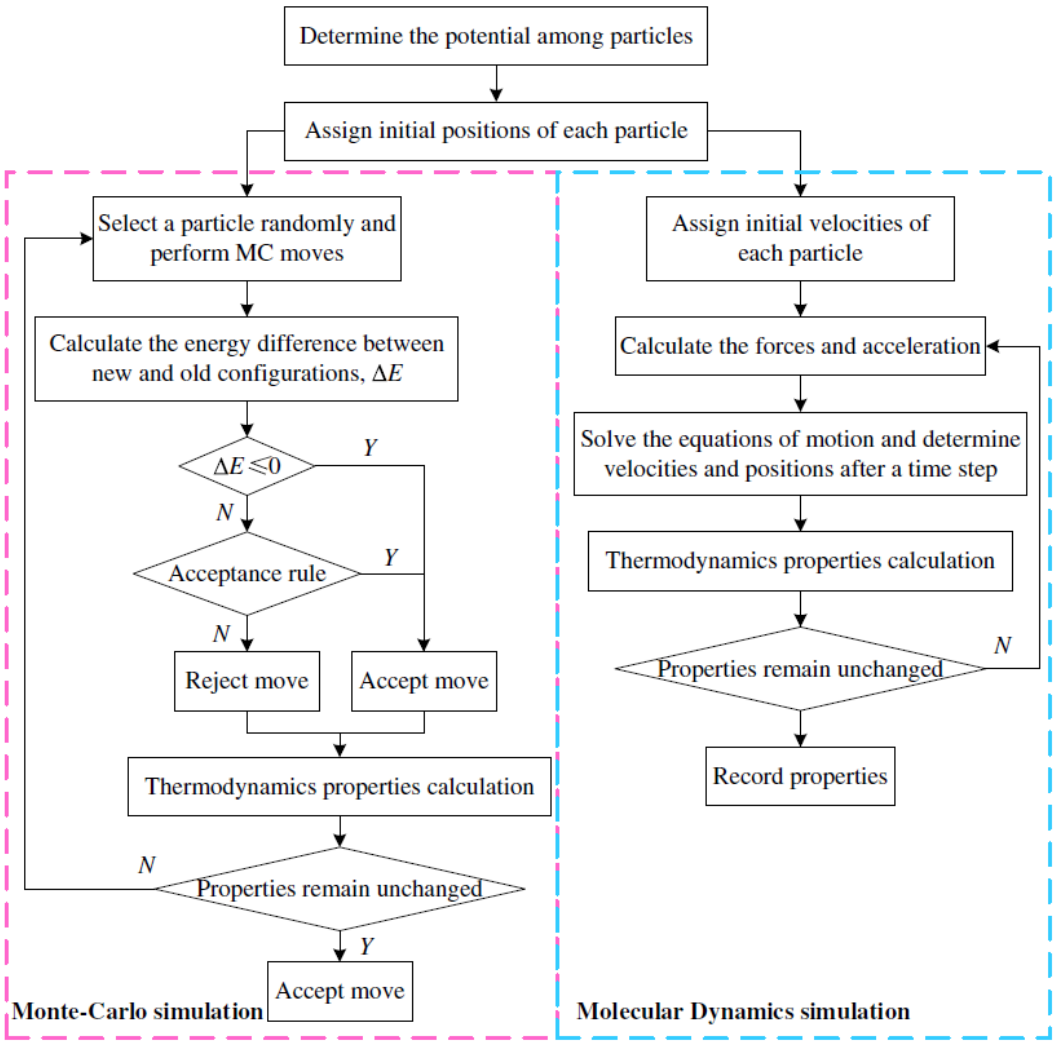

Figure 1.8: Flow chart of MC and MD simulation (Nie et al., 2018).

1.6 Aims and Objectives

The primary objective of this thesis is to introduce and investigate a novel computational technique called the DOS Partitioning MC method. The DOS partitioning method is designed to accurately calculate the phase coexistence properties of binary mixtures comprising carbon

dioxide (CO_2) as the main component and impurities such as sulfur dioxide (SO_2), hydrogen sulfide (H_2S), and nitrogen (N_2).

One of the key motivations behind this study is the increasing significance of capturing CO_2 streams in various industrial processes to mitigate greenhouse gas emissions. However, the captured CO_2 streams often contain impurities, such as SO_2, H_2S, and N_2, which can adversely affect the separation and purification processes. Therefore, it is crucial to understand the phase behavior and coexistence properties of these binary mixtures to optimize separation strategies and enhance the efficiency of CO_2 capture systems.

The DOS partitioning method offers a promising approach to tackle the challenges associated with accurately predicting the phase behavior of these complex mixtures. By leveraging the density of states concept, this method enables efficient sampling of the phase space, facilitating the calculation of various thermodynamic properties, such as VLE, critical points, and phase diagrams. The proposed research will involve the development and implementation of the DOS partitioning method, followed by extensive simulations to evaluate its accuracy and effectiveness in predicting the phase coexistence properties. Through rigorous comparisons with experimental data and existing simulation methods, we aim to demonstrate the superiority of the DOS partitioning MC method in capturing the intricate phase behavior of CO_2 binary mixtures with SO_2, H_2S, and N_2 impurities.

1.7 Thesis Outline

This thesis is organized into the following six chapters:

Chapter 1 gives a brief description of the background to CCS, which need to consider impurities in captured CO_2 and understand their thermodynamic properties, especially VLE. Obtaining VLE data traditionally relied on experiments or empirical equations of state, each with limitations. Molecular simulation techniques like MD and MC methods offer direct computation of thermodynamic properties, but calculating free energy by molecular simulation still poses a challenge.

Chapter 2 reviews the MC methods with particular attention to the canonical, isobaric-isothermal, and Gibbs ensembles and presents the move set needed to sample these ensembles. It presents new methodologies development, illustrating the direct computation of the partition function of fluids through simulations.

Chapters 3, 4 and 5 describe the DOS partitioning method as a computational tool to simulate the VLE behavior of the CO_2-SO_2, CO_2-H_2S and CO_2-N_2 three binary systems. The accuracy and reliability of the DOS partitioning method are validated by comparing the simulation results with experimental data, the PR-EOS model, and the Gibbs ensemble Monte Carlo (GEMC) method reported in the literature.

Finally, Chapter 6 ends by highlighting potential extensions and future research interests.

Chapter 2

Methodology

2.1 Synopsis

This section begins with an introduction to MC techniques, and then delves into the specifics of the GEMC method, which enables the simulation of phase equilibria and interfacial phenomena. Next, the thesis introduces the force field employed in the simulations. The force field is a crucial component as it defines the intermolecular interactions and accurately represents the behavior of the binary system under investigation. The thesis provides a comprehensive explanation of the force field parameters and the considerations taken to ensure its reliability in reproducing experimental observations. Moving forward, The DOS offers a powerful means to derive the absolute partition function, enabling the determination of thermodynamic properties and equilibria. The thesis emphasizes the importance of accurately calculating the free energy and highlights the methodology employed to obtain reliable results. Finally, the theoretical basis of the DOS partitioning method is elucidated and its implementation in simulations is described step-by-step. By employing these techniques, the research aims to enhance the understanding of VLE in binary systems and contribute to the advancement of molecular simulation methodologies in general.

2.2 Monte Carlo Methods

In the ensemble average approach, because a set of systems in the ensemble must satisfy the same macroscopic conditions, the ensemble varies in response to those conditions. It is usual

to utilize three ensembles in molecular simulation: canonical ensemble (the temperature T, number of molecules N and volume of system V are imposed), isothermal-isobaric ensemble (T, N and the pressure p of the system are imposed) and Gibbs ensemble. When the density of a monophasic fluid has been determined, the canonical ensemble may be used to simulate this fluid and to obtain some of the required properties, such as pressure, heat capacity, and chemical potential obtained using molecular simulation (Ungerer et al., 2007). Since the chemical potential of the grand-canonical ensemble is constant, it is suitable for addressing problems related to adsorptions.

By examining the partition function Q, the macroscopic thermodynamic properties of the different ensembles can be obtained. The classical expression for the partition function is:

$$Q = \frac{1}{h^{3N}N!} \iint exp[-\beta H(\boldsymbol{p}^N, \boldsymbol{r}^N)] d\boldsymbol{p}^N d\boldsymbol{r}^N \qquad (1.3)$$

where h represents Planck's constant, $N!$ is used for particles that cannot be distinguished, β is $1/k_BT$, k_B represents the Boltzmann's constant and $H(\boldsymbol{p}^N, \boldsymbol{r}^N)$ is Hamiltonian function. All particle positions $\boldsymbol{r}^N$ and conjugate momenta $\boldsymbol{p}^N$ are taken into account in the integral. When N, V, and T are fixed in the canonical ensemble, macroscopic thermodynamic properties A can be determined by the following equation:

$$A = \frac{\int A(\boldsymbol{r}^N) exp[-\beta E(\boldsymbol{r}^N)] d\boldsymbol{r}^N}{\int exp[-\beta E(\boldsymbol{r}^N)] d\boldsymbol{r}^N} \qquad (1.4)$$

In this equation, $\boldsymbol{r}^N$ represents the set of positions of N particles composing the system and $E(\boldsymbol{r}^N)$ represents the potential energy. The above Equation 1.4 can be used to calculate the thermodynamic properties of A by calculating the integrals within the numerator and denominator over particle positions ($\boldsymbol{r}^N$). The thermodynamic property A can be calculated by establishing a set of predefined coordinates and proceeding along either time (used in MD) or ensemble space (used in MC) in such a manner that the Boltzmann distribution gives the probability that the system will occur in one or more of the relevant states.

$$P[E(\boldsymbol{r}^N)] = \frac{exp[-\beta E(\boldsymbol{r}^N)]}{\int exp[-\beta E(\boldsymbol{r}^N)] d\boldsymbol{r}^N} \qquad (1.5)$$

where P is the probability that a configuration $\boldsymbol{r}^N$ is present in the system. The partition function can be calculated by

$$Q(N,V,T) = \frac{1}{N!\Lambda^{3N}} \int exp[-\beta E(\boldsymbol{r}^N)] d\boldsymbol{r}^N \qquad (1.6)$$

where Λ represents the thermal de Broglie wavelength, E represents the configurational energy of the system and $\boldsymbol{r}^N$ is a set of positions of all N particles. Therefore, the MC simulation is based on this principle.

In order to determine phase equilibrium, each phase is required to be in chemical equilibrium, which means the temperature (T), pressure (p) and chemical potential (μ) should be equal in two phases. Despite this, no such ensemble (μpT) exists due to the lack of a thorough parameter bound. To directly simulate the VLE, Panagiotopoulos (1987) proposed GEMC. The GEMC method introduces two phases without explicit interfaces but simulates each phase independently. Therefore, it is an extremely useful tool for calculating the VLE of relatively large systems. The simulation commences by constructing the vapour phase and the liquid phase within distinct boxes, namely box 1 and box 2, respectively (Panagiotopoulos, 2006). Subsequently, MC moves are executed as part of the simulation process. In order to achieve chemical equilibrium, particles are first displaced and rotated within each box. In addition, the volume of each box is adjusted in accordance with a fixed total volume to ensure that the pressure equilibrium between the two boxes is reached. Following this process, the NVT-GEMC is defined as a GEMC with a constant volume throughout the whole simulation box. Moreover, when the pressure within the entire simulation box remains unvarying, the NpT-GEMC method is employed. Finally, the transfer of particles between the two boxes is conducted to attain equilibrium chemical potential.

The partition function for NVT Gibbs ensemble can be expressed by

$$G_{Gibbs}(NVT) = \sum_{N_1=0}^{N} \frac{1}{V\Lambda^{3N} N_1!\,(N-N_1)!} \int_0^V (V-V_1)^{N-N_1} V_1^{N_1} d\,V_1 \times$$

$$\int exp\left[-\beta E\left(\boldsymbol{s}_1^{N_1}; V_1\right)\right] d\boldsymbol{s}_1^{N_1} \int exp\left[-\beta E\left(\boldsymbol{s}_2^{N-N_1}; V-V_1\right)\right] d\boldsymbol{s}_2^{N-N_1} \qquad (1.7)$$

where N and V are the total number of particles and volume of the system, N_1 and V_1 are the number of particles and volume of subsystem (cubic box) 1, and $\boldsymbol{s}_1$ and $\boldsymbol{s}_2$ are sets of reduced coordinates of subsystem 1 and 2, respectively.

For each MC moves, form a current (old) configuration (o) into a new configuration (n), the acceptance criterion for each movement, derived from the principles of statistical thermodynamics, can be mathematically represented by the following equations.

$$P_{displacement,accept} = min\left[1, \frac{w(n)}{w(o)}\right]$$

$$= min\left[1, exp\left(-\beta E\left(s^N(n)\right) - E\left(s^N(o)\right)\right)\right] \quad (1.8)$$

$$P_{volume,accept} = min\left[1, \frac{w(n)}{w(o)}\right]$$

$$= min\left[1, \left(\frac{V_1(n)}{V_1(o)}\right)^{N_1}\left(\frac{V_2(n)}{V_2(o)}\right)^{N_2} exp\left(-\beta E\left(s^N(n)\right) - E\left(s^N(o)\right)\right)\right] \quad (1.9)$$

$$P_{transfer,accept} = min\left[1, \frac{w(n)}{w(o)}\right]$$

$$= min\left[1, \frac{N_2 V_1}{(N_1+1)V_2} exp\left(-\beta E\left(s^N(n)\right) - E\left(s^N(o)\right)\right)\right] \quad (1.10)$$

where w(i) represents the weighting of the configuration i. Additionally, even though GEMC has been demonstrated to be a powerful and efficient method of estimating vapour-liquid coexistence, there are some works that have indicated that GEMC is vulnerable to low acceptance ratios when considering complex molecule systems (Nie et al., 2018). In dense phases, this limitation will be more pronounced.

2.3 Force Fields

When employing MC methods and MD simulations, it becomes essential to employ a simplified analytical potential function to characterize the intermolecular and intramolecular interactions within a system comprising a large number of atoms (Nie et al., 2018). These functions are referred to as force fields (Cornell et al., 1995). It is important to emphasize that force fields are the result of the limited understanding of molecular interactions and the limited

computational resources at present. Experiment data are predicted more precisely and closely to actual physical phenomena when a complex force field is employed. It is essential to find a balance between the complexity of the force field, the capability to establish all the parameters of the force field, and the time available for simulation. In this sense, a suitable force field represents a balance, but as computing speeds increase and sampling algorithms become more efficient, the balance may change.

In order to model single molecules or a collection of molecules, a typical force field can be represented as follows:

$$E_p(\boldsymbol{r}^N) = \sum_{bonds} \frac{k_{b_i}}{2}\left(l_i - l_{i,0}\right)^2 + \sum_{angles} \frac{k_{\theta_i}}{2}\left(\theta - \theta_{i,0}\right)^2 + \sum_{torsions} C_n\left(1 + cos(n\emptyset - \gamma)\right) + \sum_{a\epsilon A}\sum_{b\epsilon B} 4\varepsilon_{ab}\left[\left(\frac{\sigma_{ab}}{r_{ab}}\right)^{12} - \left(\frac{\sigma_{ab}}{r_{ab}}\right)^{6}\right] + \sum_{a\epsilon A}\sum_{b\epsilon B}\frac{q_a q_b}{r_{ab}} \qquad (1.11)$$

where E_p represents the potential energy of the system. It is arranged in two lines within Equation 1.11, and the first line contains terms that describe intramolecular interactions between pairs of bonded atoms, including bond stretching potentials, angle bending potentials, and torsional potentials. The second line includes terms that represent intermolecular interactions including Coulomb potentials which refer to electrostatic interactions, and Lennard–Jones terms which refer to van der Waals interactions. It is also necessary to take into account the fact that long-chain molecules contain intramolecular non-bonded energy.

Molecular simulations commonly utilize a four-component force field which describes the intramolecular and intermolecular (or external) forces encountered in a system. Although more complex force fields may contain further terms, these four components are typically present. There is the possibility of further decomposing non-bonded interactions into additive and non-additive interactions, for example. A force field is presented in this manner to assist in the parameterization process by providing a visual representation of how changes in its parameters affect its behavior.

2.4 Free Energy and Density of States

An understanding of free energy and its derivatives is necessary for the calculation of all thermodynamic properties of pure components or mixtures of different components, especially VLE properties. However, the calculation of absolute free energy F has been found to be substantially more challenging (Kofke and Cummings, 1997; Boulougouris et al., 2001) than that of other equilibrium thermodynamic properties, for example the potential energy E, which can be calculated through the use of time or ensemble averages. It is evident from this discussion that robust methods for computing absolute free energies are needed. Since the Gibbs-Duhem integration method (Agrawal and Kofke, 1995) and thermodynamic integration (Mitchell and McCammon, 1991) have been used before to calculate the free energy, there has been increasing attention paid to the density of states (Ω) for deriving the absolute partition function (Dickson et al., 2010; Christ et al., 2010; Li et al., 2016). As a consequence of the development of these methods, density of states calculations can be carried out, from which partition function as well as free energy can be obtained successively.

The free energy of a system in the canonical ensemble can be expressed using the following equation.

$$F = -k_B T ln Q(N,V,T) \qquad (1.12)$$

Equation 1.6 can be written in the form of reduced coordinates (s = r/L) that

$$Q(N,V,T) = \frac{V^N}{\Lambda^{3N} N!} \int_0^1 exp[-\beta E(\boldsymbol{s}^N)] d\boldsymbol{s}^N \qquad (1.13)$$

in which L is the cubic simulation box length and V ($V = L^3$) is the box volume. $V^N/\Lambda^{3N}N!$ refers to the ideal gas partition function that can be calculated numerically.

Therefore, we aim to calculate the excess partition function (Q_{ex}) which can be think of as the integral of the Boltzmann factor $\exp(-\beta E)$ over all phase space:

$$Q_{ex} = \int_0^1 exp[-\beta E(\boldsymbol{s}^N)] d\boldsymbol{s}^N \qquad (1.14)$$

The relationship between the probability of a configuration possessing energy E and the density of states $\Omega(E)$, where $\Omega(E) = \int_0^1 \delta\big(E - E(\boldsymbol{s}^N)\big)d\boldsymbol{s}^N$, is characterized by proportionality. Thus Q_{ex} can be calculated by

$$Q_{ex} = \frac{\int_{-\infty}^{\infty} \exp(-\beta E)\Omega(E)dE}{\int_{-\infty}^{\infty} \Omega(E)dE} \qquad (1.15)$$

The integration is performed across the entire range of potential energies accessible to the system. The excess partition function (Q_{ex}) can be calculated from the density of states $\Omega(E)$, as shown in Equation 1.15. Therefore, it is possible to compute all thermodynamic properties of the system using knowledge of the density of states $\Omega(E)$.

In addition, density of states calculations have the advantage that they are independent of temperature and can be used to determine all thermal properties instantly, regardless of the conditions. It has been shown that Wang–Landau sampling (Wang and Landau, 2001) is the first method to be successful in achieving the goal of crossing over high free energy barriers while visiting rare states with equal probability through the use of biased weights $w(\mathrm{E}) = 1/\Omega(E)$, leading to the possibility of directly calculating partition functions for continuous systems (Ning et al., 2021). Due to the limitation of this method, only the partial partition functions can be calculated for fluids (Ganzenmüller and Camp, 2007), so direct calculations for fluids partition functions remain a major challenge.

There is evidence that the nested sampling (NS) method based on Bayesian statistics, is the most promising method currently available in the field (Baldock et al., 2017; Bolhuis and Csányi, 2018). In the configurational space, a number of fixed fractions are partitioned by potential energies and uniformly sampled (Gong et al., 2019). According to Do and Wheatley (2011, 2012, 2013), the DOS partitioning method is the nested sampling method that only uses one walker. In addition to revisiting previously examined higher energy states, this technique decreases the configurational space by a fixed factor of two at each sampling energy level. Known crystal structures were also used as initial configurations (Do and Wheatley, 2016).

The direct integral approach (DIA) has since been proposed as an alternative method of calculating the partition function of condensed matter with a high degree of accuracy, which has been demonstrated by MD (Ning et al., 2019; Liu et al., 2019). DIA is shown to work about four orders more quickly than NS (Ning et al., 2019), and to have a precision approximately four times higher compared to NS in low-density systems while being nearly one order better in high-density systems (Gong et al., 2019). In the case of condensed matter under extreme conditions, using DIA can provide a more effective method for investigating thermodynamic properties (Gong et al., 2019). In addition to its speciality in high-density and high-pressure systems, DIA lacks the capacity to deal with low-density, high-temperature systems (Ning et al., 2021).

2.5 The Density of States Partitioning Method

Equation 2.1 indicates that the determination of the excess partition function relies on the availability of the density of states. Consequently, the primary aim is to compute the density of states $\Omega(E)$ in order to obtain Q_{ex}.

$$Q_{ex} = \frac{\int_{-\infty}^{\infty} \exp(-\beta E)\Omega(E)dE}{\int_{-\infty}^{\infty} \Omega(E)dE} \qquad (2.1)$$

This section describes how to discretize the energy range and, at the same time, obtain the integrated normalized density of states associated with each energy subdivision.

In light of the rapid fluctuations in the Boltzmann factor at lower energy levels, it becomes necessary to employ a more refined subdivision of the energy range (shown in **Figure 2.1**). Furthermore, the analysis of **Figure 2.1** reveals that the sole influential factor in this context is the integration of the density of states over the subdivision. Consequently, when the subdivision occurs at higher energy levels, larger subdivisions can be utilized.

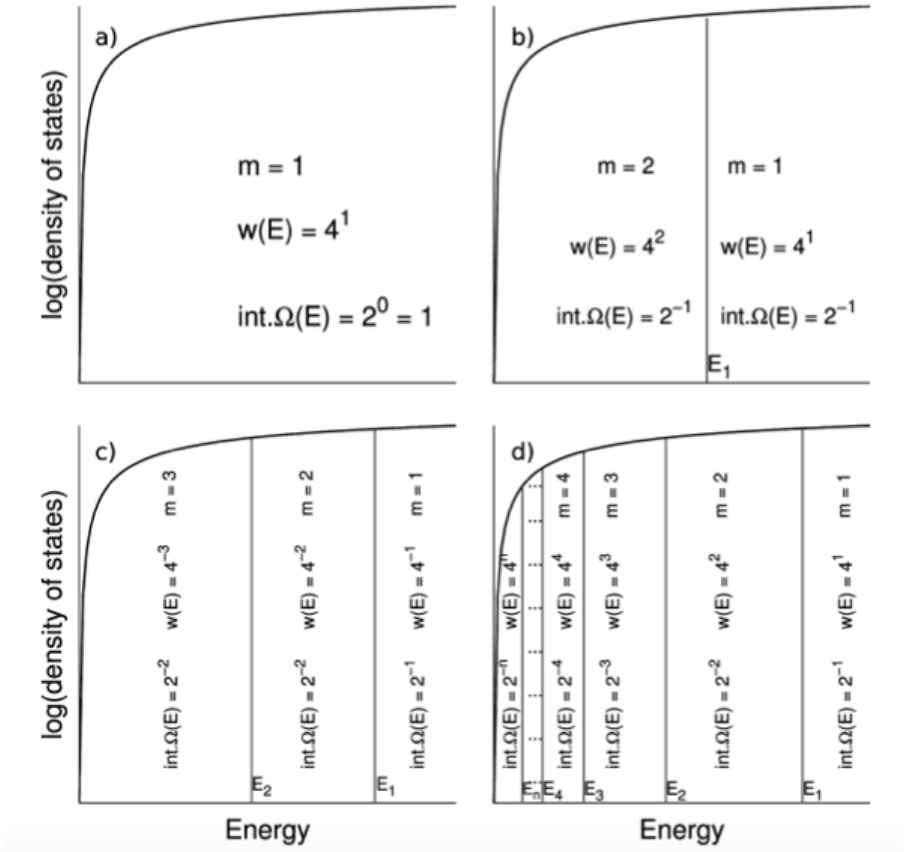

Figure 2.1. Sketch (not to scale) explaining the partitioning of the density of states (a) there is only one energy subdivision at the start of the simulation; (b) the first energy boundary E_1 divides the entire energy range; (c) the energy range is divided from -∞ to E_1 by the energy boundary E_2; and (d) after setting the n^{th} energy boundary E_n (w(E) = the weighting function and int Ω(E) = the integrated normalized density of states).

This energy range is then divided in a recursive manner in such a way as to yield the integrated normalized density of states $\int_{E_m}^{E_{m-1}} \Omega(E)\, dE / \int_{-\infty}^{\infty} \Omega(E)\, dE$ which is equal to $1/2^1$ for the first subdivision ($m = 1, E_1 \leq E \leq E_0, E_0 = \infty$) (**Figure 2.1**d). In the second partition ($m = 2, E_2 \leq E \leq E_1$), $1/2^2$ is applied, and this pattern continues iteratively until $1/2^n$ is used for the two lowest energy subdivisions ($m = n, E_n \leq E \leq E_{n-1}$ and $m = n + 1, -\infty \leq E \leq E_n$), where n represents the number of energy boundaries in the subdivision. Initially, the entire energy range is partitioned to establish the first energy boundary (E_1). Next, the energy range is divided from $-\infty$ to E_1 so that the energy boundary 2 (E_2) can be defined, and this process is repeated until reaching the energy boundary n (E_n), determined by dividing the energy range

from $-\infty$ to E_{n-1}. When the nth ($n \geq 2$) partitioning of the density of states will be accompanied by the appearance of the energy boundary E_n.

At this point, a set of MC moves for the previously occurring subdivision is performed with the weighting function w(E) $= 4^m$, which m is the subdivision to which the configurational energy E belongs ($1 \leq m \leq n$). The weighting function is an important tool in order to speed up the simulation as well as to drive the simulation down to the low energy range. Accordingly, a minimum of two-thirds of the system's configurations will be encompassed within a subdivision with the lowest energy in the current simulation. The following equation can be used as a method to estimate the probability of accepting an attempted MC move from the old configurational energy E_{old} belonging to the subdivision m_{old} to the new configurational energy E_{new} belonging to the subdivision m_{new}.

$$P(old \rightarrow new) = min\left(1, \frac{\mathrm{w}(E_{new})}{\mathrm{w}(E_{old})}\right) = min\left(1, \frac{4^{m_{new}}}{4^{m_{old}}}\right) \qquad (2.2)$$

Upon completion of all MC moves, the energy boundary E_n is set at the lowest energy subdivision of the median configurational energy ($-\infty \leq E \leq E_{n-1}$), and all sampled energy must be discarded before moving on to the next division. These procedures will be repeated in the next division energy simulation until the simulation is finished.

During the initial phase of the simulation, when there exists only a single energy subdivision, all MC moves are accepted, constituting a process referred to as random sampling (w(E) $= 4^m$). After a certain number of MC moves, the first energy boundary E_1 divides the whole energy E ($-\infty \leq E \leq \infty$) into two energy subdivisions which have the same integrated density of states ($1/2^1$ and $1/2^1$). Before proceeding to the second division of energy, all sampled energy should be discarded. Based on the second energy partitioning process, energy subdivisions 1 and 2 are weighted as 4^1 and 4^2, respectively, indicating that energy subdivision 2 has an average access frequency four times higher than energy subdivision 1. As a consequence, 1/5 of the total MC steps will be in the high-energy subdivision, and 4/5 in the low-energy subdivision. The second energy boundary E_2 is positioned at the median configurational energy of the lowest energy, following an equivalent number of MC moves as in the initial energy

partitioning. The system is then divided into three energy subdivisions, with the integrated density of states increasing exponentially for each successive subdivision: 4^1, 4^2 and 4^3. The total number of MC steps will be collected in energy partitions 1, 2 and 3, which will consist of 2/22, 4/22, and 16/22.

There is a significant increase in the density of states $\Omega(E)$ with energy, along with a significant decrease in $exp(-\beta E)$. There is a maximum value of $\int[\Omega(E)exp(-\beta E)\,dE]_{ave}$ at average energy, and it appears in Equation 2.1 to obtain Q. Since the average energy cannot be determined in advance, it is not possible to determine the number of energy boundaries. Based on the criterion used for partitioning the configuration energy, it has been determined that the integrated function $\int[\Omega(E)exp(-\beta E)\,dE]_m$ at the current energy subdivision with the lowest energy (m^{th}) is significantly smaller compared to the maximum energy subdivision among all subdivisions. At this point, further partitioning of the density of state will not yield any results, which is why the simulation can be ended. $[\int[\Omega(E)exp(-\beta E)\,dE]_m] = 10^{-9}[\int[\Omega(E)exp(-\beta E)\,dE]_{max}]$ constitutes the stopping criterion. To encompass all significant regions within the energy range, a minimum target temperature needs to be set. Due to the temperature dependency, a minimum target temperature needs being used to cover the entire energy range. From the normalized integrated density of states, the excess partition function can be determined at the end of simulation.

$$Q_{ex} = \frac{\sum_{m=1}^{m-n+1}\left(\int_{E_m}^{E_{m-1}}\Omega(E)dE\right)exp(-\beta\langle E\rangle_m)}{\sum_{m=1}^{m-n+1}\left(\int_{E_m}^{E_{m-1}}\Omega(E)dE\right)} = \frac{\sum_{m=1}^{m-n+1}2^{-m}exp(-\beta\langle E\rangle_m)}{\sum_{m=1}^{m-n+1}2^{-m}} \qquad (2.3)$$

where $\langle E\rangle_m$ is $(E_m + E_{m-1})/2$. In the first energy subdivision ($m = 1$), $\langle E\rangle_m$ equals E_1, and in the last energy subdivision, $\langle E\rangle_m$ equals E_n. Two lowest-energy subdivisions are equal in normalized integrated density of states, so 2^{-m} is replaced by 2^{-n} in the last energy subdivision. Errors generated by introducing $\langle E\rangle_m$ to this application is negligible.

By using Equation 2.3, the excess partition function can be calculated, and by using $F_{ex} = -k_B T ln Q_{ex}$, calculate the excess Helmholtz free energy (F_{ex}). A density dependent free energy for an ideal gasF_{id}can be calculated by using$F_{id} = -k_B T\left(x_{CO_2} ln\rho_{CO_2} + x_{impurity} ln\rho_{impurity}\right)$, where x represents the mole fraction and ρ is the number density. As the result, density

dependent parts of absolute free energies can be determined by summing the excess part and ideal gas components ($F = F_{ex} + F_{id}$). There is Gibbs free energy defined as G = F + pV (p represents the pressure, while V denotes the volume of the system). The pressure composition phase diagram curve is obtained by using G, and the chemical potentials of each species are derived as well. The simulation package (the code) was written and developed by Dr. Hainam Do. It is an in-house code being used within the research group (Do and Wheatley, 2011, 2012, 2013). In this thesis, I modified the force field and input files to accommodate the simulations of the report binary mixtures.

The proposed method has an advantage in allowing people to obtain the fluid's partition function and absolute free energies within a wide range of temperature and density, in which a cubic box simulation for the fluid was adopted with boundary conditions under a specific period. A spherical cut-off r_{cut} of 12 Å is utilized to truncate the Lennard-Jones interactions in this method for three of the binary mixtures. It should be noted that the cutoff length should not be larger than half length of the simulation box, therefore, those interactions beyond the cutoff will not take up the computational resources. Besides, a tail correction (Frenkel and Smit, 2002) to term r^{-6} is usually included when calculating the Lennard-Jones interactions, which gives the long-range molecule energy as:

$$E_{tail} = \frac{2}{3}\pi\rho(4\varepsilon\sigma^6)r_{cut}^{-3} \tag{2.4}$$

in which ρ represents the molecules density, ε and σ represent a depth of the well and diameter of the core, respectively. The correction for term r^{-12} is not considered as it decreases significantly with the distance. The calculation methods mentioned above have certain limitations when approaching critical points or phase boundaries. Due to the existence of finite size effects, fluctuations as well as the correlation lengths will become large and diverging near those two conditions. As for the electrostatic interactions, Ewald summation (Allen and Tildesley, 1987) was adopted in the proposed method with the tinfoil boundary condition, which is very common and widely used in research. Force-Field Parameters of the molecular models are given in **Table 2.1** below.

Table 2.1: Parameters for the 12−6 Lennard−Jones Potential and Partial Electric Charges Used in the Simulations for the Gas Molecules. * COM: centre of mass site.

Molecule	Atom	$\varepsilon/k_B\ (K)$	σ (Å)	$q\ (e)$	Angle (deg)	Bond length (Å)
CO_2	C	27.0	2.800	0.700	180.00	$l_{C=O} = 1.160$
	O	79.0	3.050	-0.350		
SO_2	S	154.4	3.585	0.470	119.50	$l_{S=O} = 1.432$
	O	62.3	2.993	-0.235		
H_2S	S	122.0	3.600	0.000	92.0	$l_{S-H} = 1.432$
	H	50.0	2.500	0.210		
	COM^*	0.0	0.000	-0.420	46.0	$l_{S-COM} = 0.300$
N_2	N	36.0	3.310	-0.482	180.00	$l_{N\equiv N} = 1.100$
	COM^*	0.0	0.000	0.964		$l_{N\equiv COM} = 0.550$

For the cross-interaction parameters, the Lorentz–Berthelot combining rules are used.

$$\sigma_{ij} = \frac{1}{2}\left(\sigma_i + \sigma_j\right) \tag{2.5}$$

$$\varepsilon_{ij} = \sqrt{\varepsilon_i\, \varepsilon_j} \tag{2.6}$$

2.6 Concluding Remarks

This chapter provides an overview of MC sampling techniques applied in various ensembles, especially the Gibbs ensembles. Subsequently, these techniques will be employed in upcoming chapters to investigate the fluid phase behavior of three binary systems: CO_2-SO_2, CO_2-H_2S and CO_2-N_2. In addition to outlining the established techniques employed in our research, this chapter introduces a new MC method that enables the computation of partition functions and free energies for fluid systems. The introduced method is notably advantageous as it provides access to free energy (hence entropy). Moreover, its simplicity and efficiency are demonstrated by the fact that energy partitioning can be completed within minutes using a single processor. Furthermore, the method encompasses a wide range of energy and temperature value.

Chapter 3

Predictions of the Vapour–Liquid Equilibria of CO_2 + SO_2 System

3.1 Synopsis

The CO_2-SO_2 binary system is of significant importance due to its relevance in various industrial processes, particularly in the context of CCS. CCS technology aims to mitigate greenhouse gas emissions by capturing CO_2 from large point sources and storing it securely underground. Understanding the VLE behavior of the CO_2-SO_2 system is crucial for optimizing the efficiency of separation processes involved in CCS. The DOS partitioning approach is utilized as a computational tool to simulate the VLE behavior of the CO_2-SO_2 binary system. The accuracy and reliability of the DOS partitioning method are validated by comparing the simulation results with the experimental ones, the PR-EOS model, and the GEMC method reported in the literature. The findings of the simulations indicate that the DOS partitioning method provides valuable insights into the VLE behavior of the CO_2-SO_2 binary system. Despite the slight overestimation of CO_2 solubility in the vapour phase at high temperatures, the overall agreement with the literature data further enhances the understanding of the other complicated system's phase behavior and solubility characteristics.

3.2 Introduction

In the field of chemical engineering, the accurate prediction and understanding of VLE are of paramount importance in the design and optimization of various industrial processes. VLE data provides essential insights into the behavior of binary mixtures, enabling engineers to make informed decisions regarding the selection of operating conditions, equipment sizing, and process efficiency. One such binary system that has garnered significant attention is the carbon dioxide-sulfur dioxide (CO_2-SO_2) system. The CO_2-SO_2 binary mixture holds considerable significance in several industrial applications, particularly in the realm of environmental control and energy production. Both carbon dioxide and sulfur dioxide are major components in numerous industrial processes, including power generation, flue gas treatment, and the production of chemicals and fuels. Understanding the VLE behavior of this system is crucial for optimizing these processes and ensuring their environmental sustainability. To develop efficient CCS processes, accurate knowledge of the VLE behavior of CO_2-SO_2 system is essential. These systems are encountered in various stages of CCS, such as the absorption of CO_2 from flue gases using SO_2-based solvents and subsequent stripping of the absorbed CO_2 for compression and storage. Predicting the CO_2-SO_2 mixtures phase behavior and equilibrium properties will aid in optimizing the performance and energy efficiency of CCS processes.

One of the primary reasons for investigating the VLE of the CO_2-SO_2 system from an industrial perspective is its relevance to CCS technologies. In recent years, there has been a growing concern over the adverse effects of greenhouse gas emissions, especially carbon dioxide, on climate change. CCS has emerged as a promising approach to mitigate these emissions by capturing CO_2 from flue gases and industrial processes and storing it underground. However, obtaining reliable experimental VLE data for the CO_2-SO_2 system presents significant challenges. The behavior of this binary mixture is influenced by several factors, including pressure, temperature, composition, and the presence of impurities. The high pressures and low temperatures at which the VLE behavior of this system is typically studied pose technical challenges for experimental measurements.

Moreover, sulfur dioxide is a toxic and hazardous gas, which limits the availability of experimental data due to safety concerns. It is difficult to perform precise measurements of VLE properties under controlled conditions due to the potential risks associated with handling and containing SO_2. These challenges contribute to the scarcity of reliable experimental data for the CO_2-SO_2 system, necessitating the development and application of alternative approaches. In light of these challenges, the use of simulation methods, such as the DOS partitioning Monte-Carlo method, has gained prominence in predicting the VLE behavior of complex binary systems. By employing this method, it becomes possible to simulate the VLE of the CO_2-SO_2 binary system and gain insights into its phase behavior, even in the absence of extensive experimental data.

Many experimental studies have investigated the VLE behavior of the CO_2-SO_2 system. In the research by Nagata et al. (2008), the CO_2-SO_2 mixture phase behavior was investigated within a cell in high-pressure equilibrium. The results showed that the solubility of CO_2 in SO_2 increases with different pressure and temperature conditions. Another study by Kudo et al. (2011) used a variable-volume view cell to measure the VLE behavior of the CO_2-SO_2 system. This study reported that the system exhibited a minimum boiling azeotrope at a condition of approximately 313 K in temperature and 6.0 MPa in pressure. Simulation methods have also been used to investigate the VLE behavior of the CO_2-SO_2 system. MD simulations have been utilized to study the phase behavior of the system by various researchers. In a study by Torres-Acosta et al. (2013), MD simulations were utilized to investigate the VLE behavior of the CO_2-SO_2 system. The results showed that the system exhibits a negative deviation from ideal behavior, with CO_2 exhibiting a preference for the liquid phase.

In this chapter, the DOS partitioning method will be adopted to predict the VLE behavior of the CO_2-SO_2 binary system. The simulations are compared with experimental data, PR-EOS model and GEMC method, which is from the literature including density, pressure and equilibrium mole fraction. By leveraging this approach, we seek to provide a comprehensive understanding of the phase behavior and equilibrium properties of this industrially significant mixture. The outcomes of this research will contribute to the design and optimization of carbon capture and

carbon storage technics and enhance our ability to tackle the challenges of greenhouse gas emissions and climate change on an industrial scale.

3.3 Results and Discussion

According to **Figure 3.1**, Gibbs free energy per particle versus volume per particle for CO_2 + SO_2 mixtures at 263.15 K, 11.056 bar, and 333.15 K, 55.65 bar are represented. As can be seen from this diagram, each phase of the system is shown to have a preference for different conditions. There is a clear tendency for the liquid phase to be favoured at 333.15K and 55.65 bar (shown in **Figure 3.1**b) when no CO_2 is present, and it is accompanied by a lower minimum value of free energy. It was found that there were two minima when the molar fraction of CO_2 was 0.4, but even in this case, the liquid phase still seemed to prevail. A gradual preference for the gas phase of CO_2 occurs as the molar fraction of CO_2 increases. In the presence of high molar fractions of CO_2, such as 0.8, the liquid phase becomes less favoured and ultimately disappears. It is noteworthy that these similar results can be obtained under different conditions as well, for example, at 263.15 K and 11.056 bar (**Figure 3.1**a).

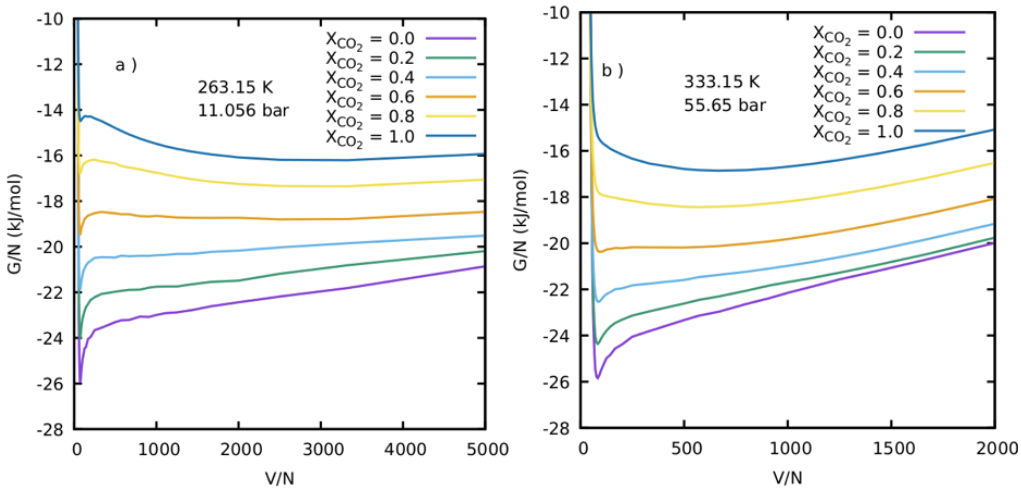

Figure 3.1: Gibbs free energy per particle versus volume per particle of CO_2 + SO_2 at different compositions: (a) 263.15 K and 11.056 bar and (b) 333.15 K and 55.65 bar. The determination of standard errors involves conducting a series of simulations for each volume. For better clarity, the plots at the compositions of CO_2 equal to 0.0, 0.2, 0.4, 0.6, and 0.8 are offset by −5, −3.5, −2.5, −1.5, and −0.5 kJ/mol, respectively.

By taking into account the minima in **Figure 3.1**, the Gibbs free energy versus the composition for both phases can be plotted in **Figure 3.2**. The coexisting composition can be found from a double common tangent connecting the two phases in **Figure 3.2**. The phase diagram for the binary mixture CO_2 + SO_2, which is taken from **Figure 3.2**, and is plotted in **Figure 3.3** with the results of the experiment (Coquelet et al., 2014), the PR-EOS model with k_{ij} = 0.0274 (Coquelet et al., 2014), and the Gibbs Ensemble Monte Carlo method (Lachet et al., 2009).

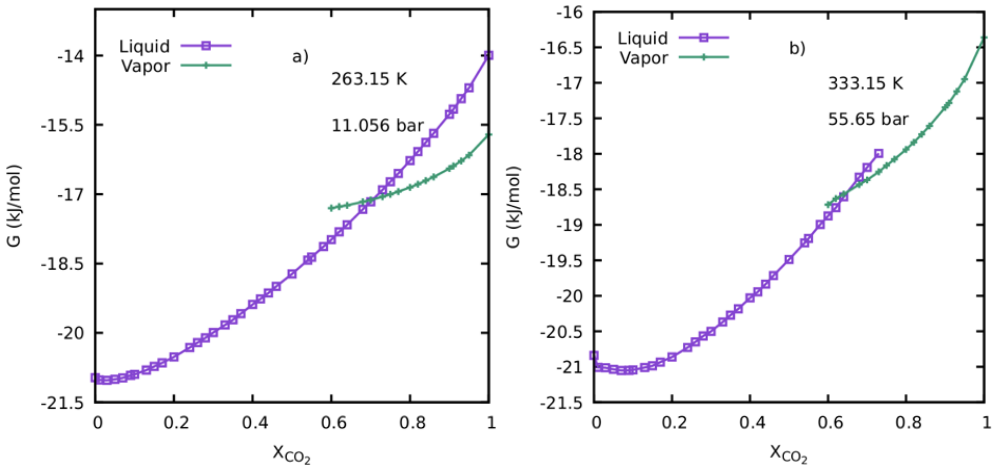

Figure 3.2: Gibbs free energy per particle versus CO_2 composition for CO_2 + SO_2: (a) 263.15 K and 11.056 bar and (b) 333.15 K and 55.65 bar. By performing a set of simulations for each volume, the standard deviations were obtained and shown as error bars.

In comparison with the literature data, there is very good agreement at both temperatures (see **Figure 3.3** a and b) with the exception of the DOS partitioning method results at high temperatures in the vapour phase. Based on the simulations conducted, it has been observed that the solubility of CO2 in the vapour phase is slightly overestimated, although this discrepancy falls within the statistical uncertainties associated with the simulations.

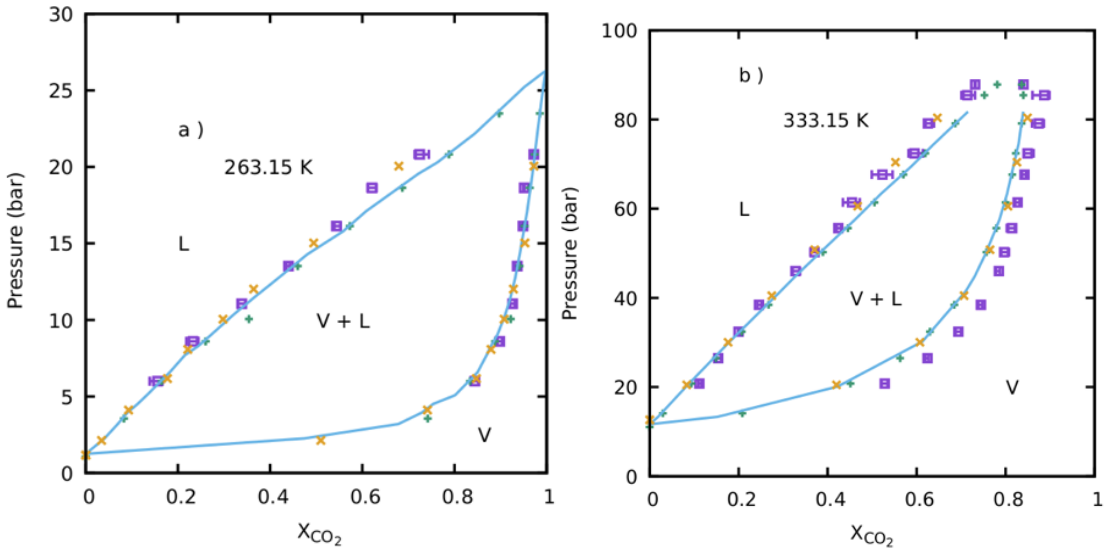

Figure 3.3: Phase diagram of the CO_2 + SO_2 system at (a) 263.15 K and (b) 333.15 K. Squares with error bars represent the DOS partitioning method results. Blue lines are the PR-EOS model with kij = 0.0274 results. Pluses represent the experimental results. Crosses represent the Gibbs Ensemble Monte Carlo method results.

The DOS partitioning approach may not accurately capture the temperature effects on the solubility of CO_2 in the vapour phase. The solubility of CO_2 in the vapour phase is known to decrease with increasing temperature, and the DOS partitioning method may not fully capture this effect. It's possible that the simulated results are overestimated due to the limitations of the DOS partitioning method in capturing the effects of temperature. The intermolecular interactions between CO_2 and SO_2 may become stronger at high temperatures. The DOS partitioning method relies on assumptions about the intermolecular interactions between the components of the binary system. It's possible that at high temperatures, the interactions between CO_2 and SO_2 become stronger and are not fully captured by the DOS partitioning method. This could lead to an overestimation of the solubility of CO_2 in the vapour phase.

If G as well as dG/dx are extracted from **Figure 3.2** then calculating the above equations, the chemical potential for each species (μ_1 and μ_2) could be determined at any composition.

$$\begin{cases} x_1^\alpha \mu_1^\alpha + x_2^\alpha \mu_2^\alpha = G^\alpha \\ dG^\alpha / dx_1^\alpha = \mu_1^\alpha - \mu_2^\alpha \end{cases} \quad (3.1)$$

in which μ represents the chemical potential and α is the phase state which can be vapour or liquid phase.

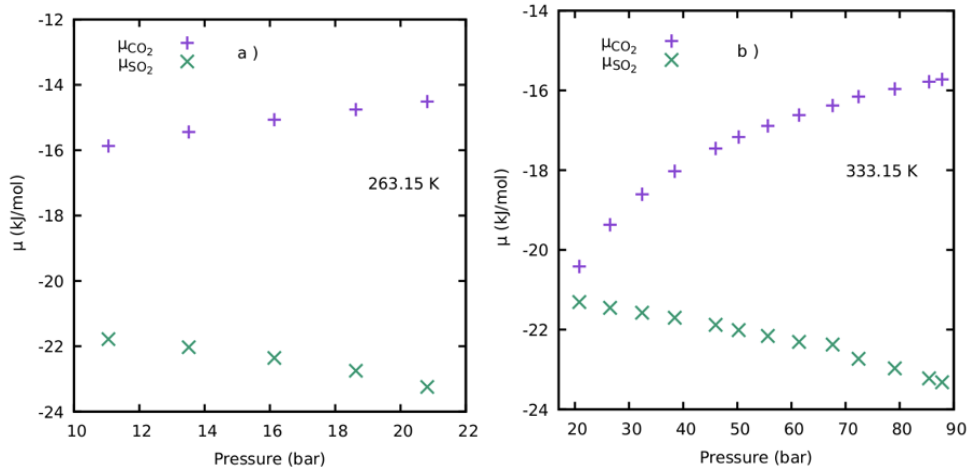

Figure 3.4: Chemical potentials of each species in the mixture CO_2 + SO_2 at the vapour−liquid equilibrium condition versus pressure at (a) 263.15 K and (b) 333.15 K.

With the help of Equation 3.1, **Figure 3.4** depicts the chemical potentials of each of the components in the CO_2 + SO_2 system at the condition of VLE. It has been demonstrated that the chemical potential of SO_2 decreases while that of CO_2 increases with increasing pressure at both temperatures. According to the graph, it can be concluded that the chemical potential of SO_2 is about as sensitive to pressure as the chemical potential of CO_2, when the chemical equilibrium between the two phases is reached.

3.4 Conclusion

The DOS partitioning method was employed as a computational tool to simulate the VLE behavior, and the accuracy and reliability of this method were validated through the comparation of the results with the experimental data, the PR-EOS model, and the GEMC method from the literature. The findings of the simulations have provided valuable insights into the VLE behavior of the CO_2-SO_2 system. Overall, the DOS partitioning method demonstrates good agreement with the literature data, thereby enhancing people's understanding of the phase behavior and solubility characteristics of this complex system. It accurately predicts the solubility of CO_2 in the liquid phase and the vapour phase at lower temperatures. However, at

high temperatures, there is a slight overestimation of CO_2 solubility in the vapour phase. The outcomes of this research contribute to the efficient design and optimization of separation processes involved in CCS. By understanding the VLE behavior of the CO_2-SO_2 binary system, we can enhance the effectiveness of capturing CO_2 from large point sources and storing it securely underground. The insights gained from this study can aid in the development of more robust and cost-effective CCS technologies, ultimately helping to mitigate greenhouse gas emissions and combat climate change.

Future research could focus on refining the DOS partitioning method to improve its accuracy at high temperatures. Additionally, exploring the VLE behavior of other binary and multicomponent systems relevant to CCS could expand our knowledge and further optimize separation processes. By continuing to advance our understanding of these systems, we can continue to develop sustainable solutions for reducing greenhouse gas emissions and promoting a cleaner and greener future.

Chapter 4

Predictions of the Vapour–Liquid Equilibria of CO_2 + H_2S System

4.1 Synopsis

The CO_2-H_2S binary system is relevant to sour gas treatment, where the separation of CO_2 and H_2S from natural gas or flue gas is of utmost importance. Understanding the VLE behavior of this system contributes to the development of efficient and environmentally sustainable sour gas treatment processes, ensuring compliance with regulatory requirements and minimizing environmental impact. This chapter investigates the VLE of the CO_2-H_2S binary system using the DOS partitioning method. By comparing the simulation results with both experimental data and the PR-EOS model from the literature, valuable insights into the phase behavior of the system are obtained. The comparative analysis reveals that, in contrast to the CO_2-H_2S binary system, the CO_2-H_2S binary system exhibits a smaller width of the two-phase region. Moreover, the simulation results indicate that the DOS partitioning method slightly overestimates the solubility of CO_2 in both the liquid and vapour phases at both temperatures. Although this discrepancy exists, it remains within acceptable limits considering the statistical uncertainties inherent in the simulations.

4.2 Introduction

The investigation of VLE in binary mixtures plays a crucial role in the field of chemical engineering, enabling the design and optimization of various industrial processes. Among the binary systems of interest, the carbon dioxide-hydrogen sulfide (CO_2-H_2S) mixture holds

significant importance, particularly in the realm of energy production, environmental control, and the oil and gas industry. Understanding the VLE behavior of this system is essential for addressing industrial challenges and ensuring the safe and efficient operation of processes.

The CO_2-H_2S binary system has garnered substantial attention due to its relevance to several industrial applications. Carbon dioxide is a byproduct of various processes, including power generation, industrial emissions, and the production of chemicals and fuels. On the other hand, hydrogen sulfide is encountered in natural gas streams and oil refining processes, and its removal is vital for ensuring product quality and meeting environmental regulations. Consequently, accurate knowledge of the VLE behavior of the CO_2-H_2S system is essential for optimizing these processes and ensuring their sustainable and cost-effective operation.

From an industrial perspective, the study of CO_2-H_2S VLE is particularly relevant to sour gas treatment processes. Sour gas, which contains high concentrations of hydrogen sulfide, poses significant challenges in the oil and gas industry. It is necessary to remove H_2S from the gas stream to meet safety standards, prevents corrosion in pipelines and equipment, and produce marketable natural gas. The VLE behavior of the CO_2-H_2S system plays a crucial role in designing efficient and reliable sour gas treatment processes, including gas sweetening operations. Obtaining reliable experimental VLE data for the CO_2-H_2S system presents notable challenges. The behavior of this binary mixture is influenced by factors such as pressure, temperature, composition, and the presence of impurities. Experimental measurements of VLE properties under controlled conditions are complicated by the high pressures and low temperatures typical in sour gas treatment processes. Additionally, hydrogen sulfide is a toxic and hazardous gas, making experimental measurements difficult due to safety concerns.

Simulation approaches have gained prominence in addressing this challenge, offering a means to estimate phase equilibria in the absence of extensive experimental data. In recent years, DOS partitioning method has emerged as a powerful simulation method for predicting VLE properties of fluid systems. DOS partitioning method combines the efficiency of GEMC simulations with the accuracy of DOS partitioning techniques. It has been successfully applied to study the VLE behavior of various fluid systems.

In this chapter, we use DOS partitioning method to study the VLE behavior of the CO_2-H_2S binary system. We aim to provide accurate and reliable predictions for the equilibrium properties of the system, including vapour and liquid compositions, densities, and phase coexistence conditions. The outcomes of this research will contribute to the design and optimization of sour gas treatment processes, improving operational efficiency, and ensuring compliance with environmental regulations. Ultimately, the insights obtained from this study will facilitate safer and more sustainable operations in the oil and gas industry.

4.3 Results and Discussion

The pressure-composition diagram for the binary mixture CO_2 + SO_2, which is also taken from the plot of the Gibbs free energy per particle versus volume per particle for binary mixtures (**Figure 4.1**), and is plotted in **Figure 4.2** based on the results of the experiment (Chapoy, et al., 2013; Bierlein and Kay, 1953) and the PR-EOS model with k_{ij} = 0.095 (Chapoy, et al., 2013). The width of the two-phase region of this mixture is smaller than that of the CO_2 + SO_2 binary mixture. In both temperature regimes, the simulations demonstrate a slight overestimation of the solubility of CO_2 in the liquid and vapour phase.

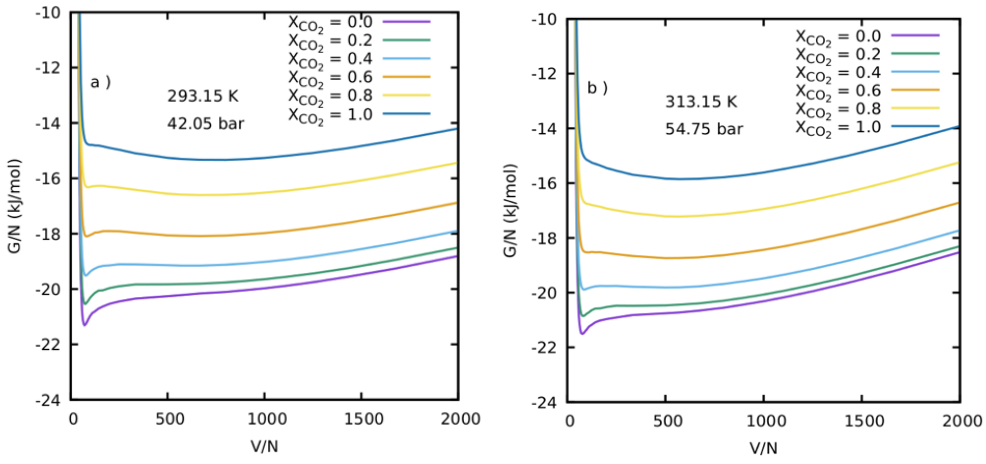

Figure 4.1: Gibbs free energy per particle versus volume per particle of CO_2 + H_2S at various compositions: (a) 293.15 K and 42.05 bar and (b) 313.15 K and 54.75 bar. The determination of standard errors involves conducting a series of simulations for each volume.. In most cases, the errors in G/N are between 0.4% and 0.7%. For better clarity, the plots at the compositions

of CO_2 equal to 0.0, 0.2, 0.4, 0.6, and 0.8 are offset by −5, −3.5, −2.5, −1.5, and −0.5 kJ/mol, respectively.

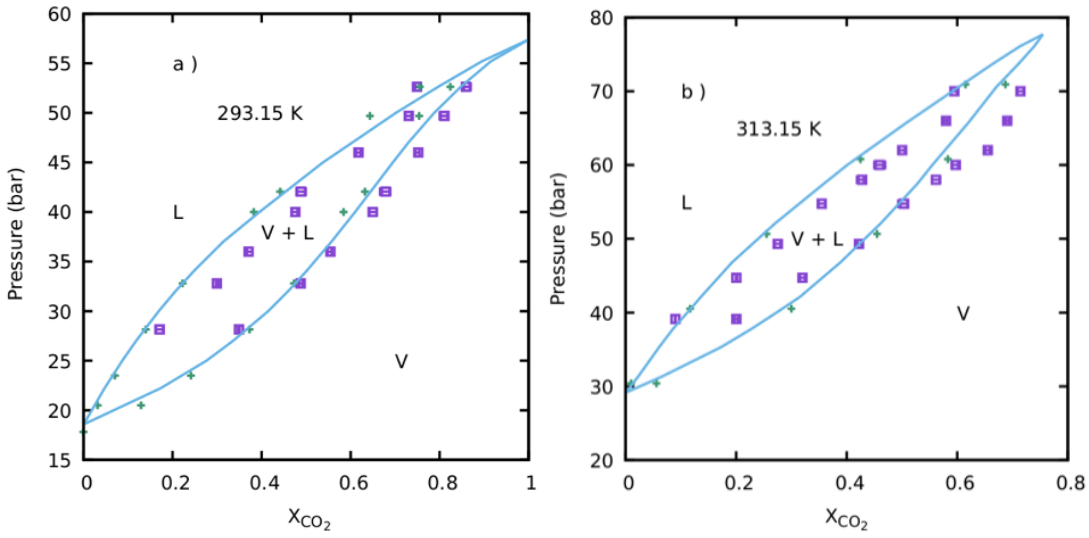

Figure 4.2: VLE of the binary system CO_2 + H_2S at (a) 292.15 K and (b) 313.15 K. Squares with error bars represent the DOS partitioning method results. Blue lines are the PR-EOS model with k_{ij} = 0.095 results. Pluses in (a) represent the experimental results from Chapoy, et al. (2013). Pluses in (b) represent the experimental results from Bierlein and Kay (1953).

The accuracy of the DOS partitioning method in predicting the phase behavior of binary mixtures relies on multiple factors, such as the accuracy of the force field and the simulation parameters. According to the VLE of the CO_2-H_2S binary system in **Figure 4.2**, the results generated by DOS partitioning method may not be as accurate as other CO_2 binary systems for several reasons:

Firstly, the CO_2-H_2S binary system is more complex than some other CO_2 binary systems, as it involves both dipole-dipole and quadrupole-dipole interactions. The accuracy of the force field used in the DOS partitioning method can be affected by the complexity of intermolecular interactions, and if the force field is not accurate enough to account for these interactions, the predicted phase behavior may deviate from experimental results. Secondly, the CO_2-H_2S binary system has limited experimental data available for validating the predictions of the DOS partitioning method. This can make it more difficult to accurately determine the simulation

parameters and force field parameters, which can result in deviations between the predicted and experimental phase behavior.

Thirdly, the accuracy of DOS partitioning method can be influenced by various simulation conditions, such as temperature and pressure. Among binary systems, the CO_2-H_2S system may have a narrower range of conditions in which it is in thermodynamic equilibrium, which poses challenges for obtaining accurate predictions of its phase behavior. Typically, natural gas processing conditions, where CO_2 and H_2S are common impurities, are of interest. For instance, at low temperatures and low pressures, the CO_2-H_2S system is anticipated to exist in the vapour phase, and its phase behavior is usually described well by the ideal gas law. However, at elevated pressures and temperatures, the system may exhibit non-ideal behavior, such as molecular clustering or association, resulting in deviations from the ideal gas law. At low temperatures and high pressures, the system may undergo phase transitions, such as solidification or clathrate formation, which can negatively impact the accuracy of DOS partitioning method. Furthermore, the force field used in the DOS partitioning method may also be influenced by the simulation conditions. For instance, at high pressures, the intermolecular interactions become stronger, leading to greater molecular packing and a higher likelihood of non-ideal behavior. As a result, discrepancies between predicted and experimental phase behavior may occur.

Moreover, the DOS partitioning method has certain limitations and may not be suitable for all types of mixtures. The method assumes that the molecules interact through a pairwise potential, which may not accurately depict the interactions in all mixtures. Furthermore, the DOS partitioning method may not be applicable to mixtures with strong polar interactions or hydrogen bonding.

Overall, due to the complexity of intermolecular interactions, limited force field parameters, limited experimental data, and high pressures and temperatures, the accuracy of the DOS partitioning method in predicting the VLE of the CO_2-H_2S binary system may be lower than that of other CO_2 binary systems.

The width of the two-phase region in the VLE of the CO_2-H_2S binary system is generally narrower than other CO_2 binary systems due to the unique properties of H_2S. H_2S is a polar molecule with a larger molecular size than CO_2, which can affect the intermolecular interactions and phase behavior of the mixture. In general, the width of the two-phase region in a binary system is determined by the difference in the vapour pressures of the two components, which is affected by the intermolecular interactions between the molecules. For example, in the CO_2-methane binary system, the two-phase region is relatively wide because CO_2 and methane have weak intermolecular interactions and similar molecular sizes. In contrast, in the CO_2-water binary system, the two-phase region is narrow due to the strong intermolecular interactions between CO_2 and water. In the CO_2-H_2S binary system, the intermolecular interactions between CO_2 and H_2S are intermediate in strength, and their molecular sizes are significantly different. As a result, the width of the two-phase region is narrower than other CO_2 binary systems. This can be seen in experimental measurements and simulations of the CO_2-H_2S binary system, where the two-phase region is observed to be relatively narrow, even at high pressures. Additionally, the polar nature of H_2S can affect the distribution of the molecules between the vapour and liquid phases. H_2S molecules tend to prefer the liquid phase due to the strong intermolecular interactions with water molecules, which can reduce the vapour pressure and narrow the two-phase region further.

In summary, the narrower width of the two-phase region in the VLE of the CO_2-H_2S binary system compared to other CO_2 binary systems can be attributed to the intermediate intermolecular interactions between CO_2 and H_2S and the polar nature of H_2S, which affects the distribution of the molecules between the vapour and liquid phases.

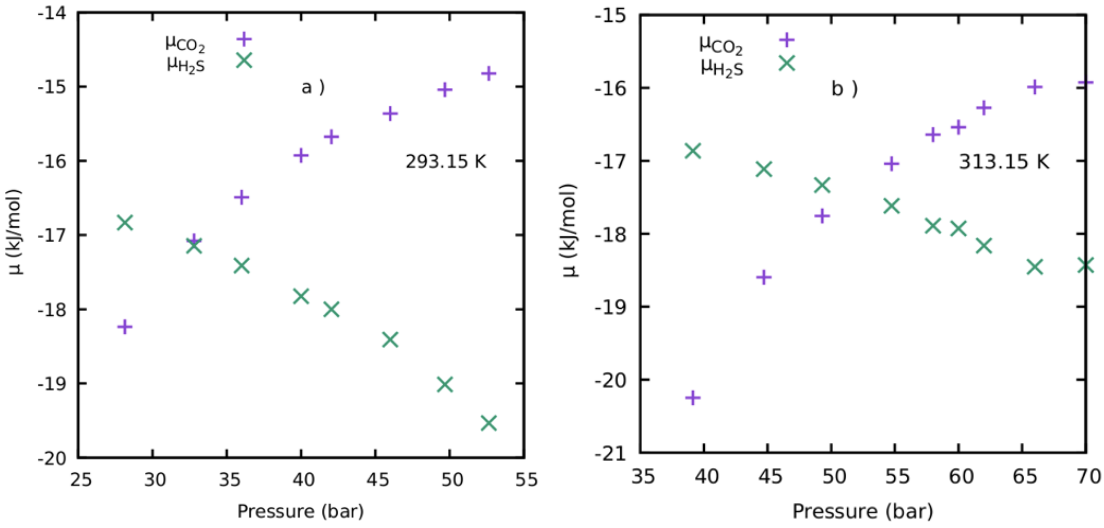

Figure 4.3: Chemical potentials of each species in the mixture CO_2 + H_2S at the vapour-liquid equilibrium condition versus pressure at (a) 293.15 K and (b) 313.15 K.

It has been observed at both two temperatures, the H_2S chemical potential decreases with increasing pressure, whereas the chemical potential of CO_2 increases (see **Figure 4.3**). Consequently, it can be concluded that the chemical potential of H_2S is about as sensitive to pressure as the chemical potential of CO_2, when the chemical equilibrium between the two phases is reached.

4.4 Conclusion

This chapter focused on investigating the VLE behavior of the CO_2 + H_2S binary system, which is crucial for sour gas treatment processes. Sour gas treatment involves the separation of CO_2 and H_2S from natural gas or flue gas, and understanding the VLE behavior of this system is essential for the development of efficient and environmentally sustainable treatment processes. The DOS partitioning method was employed as a computational tool to simulate the VLE behavior of the CO_2 + H_2S binary system. The simulation results were compared with experimental data and the PR-EOS model from the literature, providing insights into the system's phase behavior.

The comparative analysis revealed that the CO_2 + H_2S binary system exhibits a smaller width of the two-phase region compared to the CO_2 + H_2S binary system. This difference is important

in designing separation processes as it affects the operational conditions and efficiency of the treatment system. Furthermore, the simulation results indicated that the DOS partitioning method slightly overestimates the solubility of CO_2 in both the liquid and vapour phases at different temperatures. However, it is important to note that this discrepancy falls within acceptable limits considering the statistical uncertainties inherent in the simulations.

The findings of this research contribute to the development of efficient and environmentally sustainable sour gas treatment processes. By understanding the VLE behavior of the $CO_2 + H_2S$ binary system, we can optimize the design and operational parameters of separation processes, ensuring compliance with regulatory requirements and minimizing the environmental impact. Future research could focus on investigating the VLE behavior of other relevant binary or multicomponent systems in sour gas treatment could further enhance our understanding and improve the efficiency of treatment processes.

Overall, the insights gained from this study contribute to the development of sustainable solutions for sour gas treatment, promoting environmental stewardship and ensuring the responsible utilization of natural resources.

Chapter 5

Predictions of the Vapour–Liquid Equilibria of CO_2 + N_2 System

5.1 Synopsis

The CO_2-N_2 binary system holds significant importance in various industrial and chemical processes, particularly in the field of gas separation and purification. Understanding the VLE behavior of this system is crucial for optimizing the efficiency of separation processes used in applications such as natural gas treatment and flue gas purification. This chapter focuses on utilizing the DOS partitioning method to investigate the VLE behavior of the CO_2-N_2 binary system. The primary objective is to compare the simulation results with experimental data and existing literature models, assessing the reliability and accuracy of the DOS partitioning method. The simulations demonstrate reasonable agreement with the literature data for the vapour phase, particularly at low temperatures. Notably, at high temperatures, the DOS partitioning method simulations slightly overestimate the mole fraction of N_2 in the vapour phase. Nevertheless, these deviations remain comfortably within the statistical uncertainties inherent to the simulations and demonstrate a reasonable agreement with the available literature data.

5.2 Introduction

In carbon capture and storage, CO_2 is captured from industrial processes and stored underground in geological formations. However, the CO_2 captured is often mixed with other gases, such as N_2, which can reduce the purity of the stored CO_2. Therefore, it's important to

understand the VLE of the CO_2-N_2 binary system in order to effectively separate and store the CO_2. VLE refers to the state where the rates of evaporation and condensation of a liquid are in balance. In the CO_2-N_2 binary system, the VLE is influenced by factors such as temperature, pressure, and the composition of the mixture. To separate CO_2 from N_2 in a carbon capture and storage system, the VLE can be exploited through a process called absorption. This involves dissolving the CO_2 and N_2 mixture in a solvent, such as an amine solution, which preferentially absorbs the CO_2. The solvent is then regenerated, releasing the CO_2 in a pure form for storage. It is worth noting that the separation of CO_2 from N_2 is more difficult than the separation of CO_2 from H_2S, as the difference in their vapour pressures is much smaller. This means that more energy and resources may be required to effectively separate CO_2 from N_2 in a carbon capture and storage system. Overall, understanding the VLE of the CO_2-N_2 binary system is imperative in designing efficient and effective carbon capture and storage systems.

Molecular modeling through computer simulation offers a valuable means of predicting the VLE behavior of fluid systems across a broad spectrum of conditions, while also granting insights into their underlying microscopic structure. Additionally, simulation techniques have the capability to simulate conditions that are characterized by the absence or unavailability of experimental data. Several methodologies have been proposed to address these objectives, including the NpT + test particle method, grand canonical ensemble Monte Carlo with histogram reweighting, Gibbs-Duhem integration, and the GEMC approach. In this chapter, we specifically investigate the accuracy of molecular simulations employing the DOS partitioning method for determining the VLE of the CO_2-N_2 binary system.

5.3 Results and Discussion

The pressure-composition diagram for the binary mixture CO_2 + N_2, which is taken from the plot of the Gibbs free energy versus the composition for both phases, and is plotted in **Figure 5.1** with the results of the experiment (Al-Sahhaf et al., 1983), the PR-EOS model (Fandin˜o et al., 2015) and the Gibbs ensemble Monte Carlo technique (Li et al., 2012). The simulations at both temperatures underestimate the mole fraction of N_2 in the liquid phase. A satisfactory concurrence is observed between the generated data and literature data for the vapour phase at

low temperatures. The DOS partitioning method simulations at high temperature slightly overestimate the mole fraction of N_2 in the vapour phase. These values, however, are quite well congruent with the literature data, even within the uncertainties of the simulations.

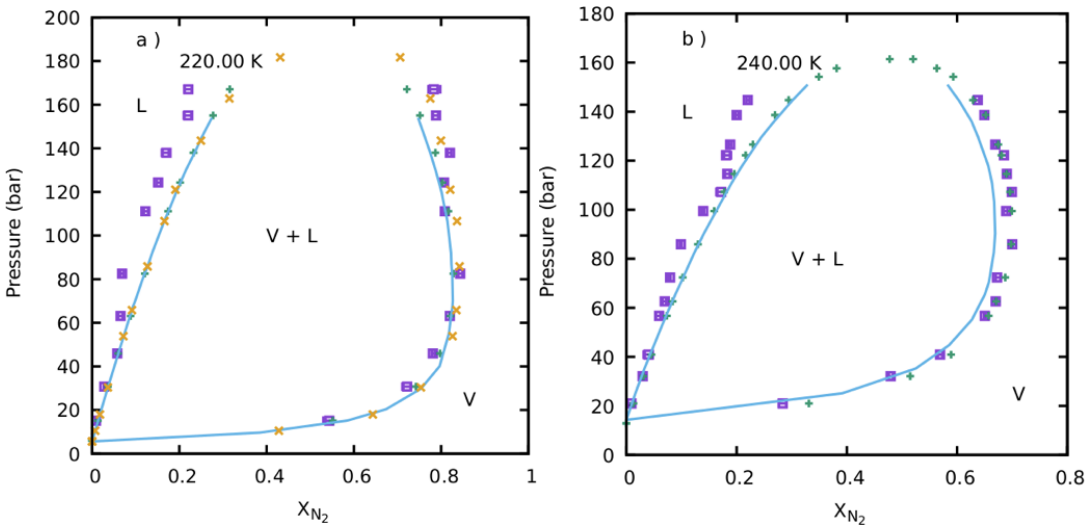

Figure 5.1: Phase diagram of the CO_2 + N_2 system at (a) 220.00 K and (b) 240.00 K. Squares with error bars represent the DOS partitioning method results. Blue lines are the PR-EOS model results. Pluses represent the experimental results. Crosses in (a) are the Gibbs ensemble Monte Carlo technique results.

It has been observed at both temperatures, that the chemical potential of N_2 increases rapidly with increasing pressure, whereas the chemical potential of CO_2 increases slowly (see **Figure 5.2**). Pressure leads to a decrease in the gradient of the chemical potential of N_2. According to the graph, it can be observed that N_2 will respond more sensitively to pressure than CO_2 at the condition of vapour-liquid equilibrium and that N_2 becomes more soluble in the mixture with increasing pressure.

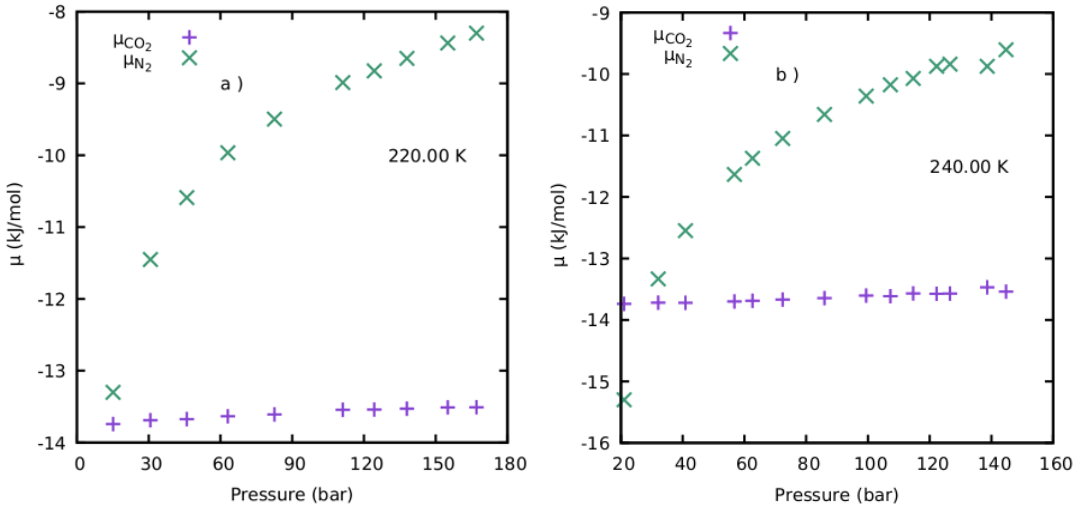

Figure 5.2: Chemical potentials of each species in the mixture $CO_2 + N_2$ at the vapour-liquid equilibrium condition versus pressure at (a) 220.00 K and (b) 240.00 K.

The DOS partitioning method is a computational technique used to predict the phase behavior of substances under various conditions. The method relies on a force field that describes the intermolecular interactions between molecules in the substance. The accuracy of the force field decreases as the pressure increases, leading to larger deviations between the experimental and predicted phase behavior. Furthermore, the DOS partitioning method assumes that the substance is in thermodynamic equilibrium and that the simulation accurately represents the conditions of the experimental system. At high pressures, however, the assumption of equilibrium may not be valid, as the system may be kinetically trapped in a metastable state, leading to deviations from the predicted behavior.

Overall, the limitations of the DOS partitioning method at high pressures are due to the increased strength of intermolecular interactions, the limitations of the force field, and the assumption of thermodynamic equilibrium. These factors can lead to larger differences between the experimental and predicted phase behavior, particularly at high pressures.

5.4 Conclusion

This thesis focused on investigating the VLE behavior of the $CO_2 + N_2$ binary system, which plays a crucial role in gas separation and purification processes. An understanding of this

system's VLE behavior is essential for the design and optimization of separation processes used in various industrial applications, including natural gas treatment and flue gas purification. The DOS partitioning method was employed as a computational tool to simulate the VLE behavior of the $CO_2 + N_2$ binary system. The primary objective was to evaluate the dependability and precision of this method through a comparative analysis of the simulation results with experimental data and established literature models. The simulations conducted in this study showed reasonable agreement with the literature data, particularly for the vapour phase at low temperatures. However, at high temperatures, the simulations slightly overestimated the mole fraction of N_2 in the vapour phase. Nevertheless, these discrepancies were within the statistical uncertainties inherent in the simulations and aligned reasonably well with the literature data.

The findings of this research contribute to the understanding of the VLE behavior of the $CO_2 + N_2$ binary system and have implications for the design and optimization of gas separation and purification processes. By improving knowledge of this system, we can enhance the efficiency and effectiveness of applications such as natural gas treatment and flue gas purification. These processes play a vital role in ensuring the quality and purity of gases used in various industries while minimizing environmental impact. Future research could focus on refining the DOS partitioning method to improve its accuracy, particularly at high pressure. Additionally, exploring the VLE behavior of other binary or multicomponent systems relevant to gas separation and purification would further expand our understanding and contribute to the development of more efficient separation processes.

Overall, this research contributes to the advancement of gas separation and purification technologies, promoting sustainable industrial practices and environmental stewardship. By optimizing these processes, we can enhance resource utilization, reduce emissions, and foster a greener and more sustainable future.

Chapter 6

Conclusion

To accurately simulate all of the sub-processes of CCS, VLE data of CO_2 mixtures are essential. A traditional method of obtaining such data has been to conduct experiments or to use empirical equations of state. It is often time-consuming and expensive to investigate a large number of different compositions and thermodynamic conditions during an experiment. However, only a limited amount of experimental data is available for calibrating equations of state models. In this thesis, the phase diagrams of binary mixtures CO_2 + SO_2, CO_2 + H_2S and CO_2 +N_2 were computed using the DOS partitioning MC technique based on standard force fields from the literature. The vapour–liquid equilibrium data from the DOS partitioning method are compared with available experimental data, equation of state modelling, and GEMC method. Overall, an excellent agreement between experiments, EOS modelling, MC simulations and DOS partitioning method is observed except for the binary mixture CO_2 + H_2S. According to the results generated in the binary mixture CO_2 + H_2S, the simulations indicate a minor overestimation of the solubility of H_2S in both phases at both temperatures due to the small width of the two-phase region. Despite this, the deviations remain within the range of statistical uncertainties associated with simulations. In general, the chemical potential of SO_2 and H_2S decreases with increasing pressure, whereas the chemical potential of CO_2 increases. When the chemical equilibrium between two phases is reached, SO_2 and H_2S have a chemical potential that is about as sensitive to pressure as CO_2. In binary mixture CO_2 +N_2, a present in CCS. The rapid increase in N_2's chemical potential occurs with increasing pressure, whereas CO_2's chemical potential rises slowly. Observations have shown that at the equilibrium condition of vapour-liquid, the impact of pressure is more pronounced for N_2 compared to CO_2, and N_2 is

more soluble in CO_2 the higher the pressure. The DOS partitioning method can be used to simulate the thermodynamic properties of of additional CO_2 mixtures that contain impurities.

Reference List

1. Abbott, M.M., 1979. Cubic Equations of State: An Interpretive Review. *Equations of stat e in engineering and research*. Washington, DC, American Chemical Society. Available a t: https://pubs.acs.org/doi/10.1021/ba-1979-0182.ch003 (Access date: 15/07/2022)

2. Allen, M.P. & Tildesley, D.J., 2017. Computer simulation of liquids. Second editi on. Oxford, United Kingdom, Oxford University Press. Available at: https://academ ic.oup.com/book/27866 (Access date: 28/08/2022)

3. Admos O. C., David Hulme., Lauchlan T, M., 2019. The 'New' national development pla nning and global development goals: Processes and partnerships. World Development, vo l 120, pp 76-89. Available at : https://www.sciencedirect.com/science/article/pii/S030575 0X19300713(Access date: 27/06/2022)

4. A.Z. Panagiotopoulos, 1987. Direct determination of phase coexistence properties of flui ds by Monte Carlo simulation in a new ensemble, *Mol. Phys.* 61, pp 813–826. Available a t: https://www.tandfonline.com/doi/abs/10.1080/00268978700101491 [Access date: 28/0 8/2022]

5. A.Z. Panagiotopoulos, 2006. Direct determination of fluid phase equilibria by simulation in the Gibbs ensemble: a review. *Molecular Simulation*. Vol 9, pp 1–23. Available at: http s://www.tandfonline.com/doi/abs/10.1080/08927029208048258 [Access date: 26/08/202 2]

6. Alder, B. J.; Wainwright, T. E., 1957. Phase Transition for a Hard Sphere System, *J. Che m. Phys.*, 27, 1208. Available at: https://aip.scitation.org/doi/pdf/10.1063/1.1743957(Acc ess date: 17/08/2022)

7. Bolhuis, P.G.; Csányi, G., 2018. Nested Transition Path Sampling. *Phys. Rev. Lett.* Vol 12 0, 250601. Available at: https://journals.aps.org/prl/abstract/10.1103/PhysRevLett.120.25 0601(Access date: 17/08/2022)

8. Baldock, R.J.; Bernstein, N.; Salerno, K.M.; Pártay, L.B.; Csányi, G., 2017. Constant-pressure nested sampling with atomistic dynamics. *Phys. Rev*., vol 96, 043311. Available at: https://journals.aps.org/pre/abstract/10.1103/PhysRevE.96.043311(Access date: 09/08/2022)

9. Boulougouris GC, Economou IG, Theodorou DN. 2001. Calculation of the chemical potential of chain molecules using the staged particle deletion scheme. *J Comput Phys*. Vol 115, 8231–8237. Available at: https://aip.scitation.org/doi/10.1063/1.1405849 [Access date: 29/08/2022]

10. B. Metz, O. Davidson, H.C. de Coninck, M. Loos, L.A. Meyer, 2005. IPCC Special Report on CO2 Capture and Storage, Cambridge University Press, Cambridge, United Kingdom. ISBN 978-0-521-68551-1. Available at: https://www.ipcc.ch/report/carbon-dioxide-capture-and-storage/ (Access date: 04/07/2022)

11. Becker, S., Bouzdine-Chameeva, T., Jaegler, A., 2020. The carbon neutrality principle: a case study in the French spirits sector. Journal of Cleaner Production. Vol 274, 122739. Available at: https://www.sciencedirect.com/science/article/pii/S0959652620327864?via%3Dihub (Access date: 30/06/2022)

12. Bobbo, S., Stryjek, R., Elvassore, N. & Bertucco, A., 1998. A recirculation apparatus for vapor-liquid equilibrium measurements of refrigerants. Binary mixtures of R600a, R134a and R236fa. *Fluid phase equilibria*. 1998 Amsterdam, Elsevier Science. pp. 343–352. https://www.sciencedirect.com/science/article/abs/pii/S0378381298003343(Access date: 14/07/2022)

13. Chen, J.-.X., Hu, P., Chen, Z.-.S., 2008. Study on the interaction coefficients in PR equation with vdW mixing rules for HFC and HC binary mixtures. *Int. J. Thermophys* 29 (6), 1945–1953. Available at: https://link.springer.com/article/10.1007/s10765-008-0528-4 (Access date: 02/08/2022)

14. Coquelet, C., Valtz, A. & Arpentinier, P., 2014. Thermodynamic study of binary a nd ternary systems containing CO2+impurities in the context of CO2 transportatio n. Fluid phase equilibria. 382, 205–211. Available at: https://www.sciencedirect.com/science/article/abs/pii/S0378381214004889 (Access date: 28/08/2022)

15. Cismondi Duarte, M., Galdo, M.V., Gomez, M.J., Tassin, N.G., Yanes, M., 2014. High pr essure phase behavior modeling of asymmetric alkane+alkane binary systems with the R KPR EOS. Fluid Phase Equilib. 362, 125–135. Available at: https://www.sciencedirect.com/science/article/abs/pii/S0378381213005463 (Access date: 02/08/2022)

16. Chapoy, A., Coquelet, C., Liu, H., Valtz, A. & Tohidi, B., 2013. Vapour–liquid equilibriu m data for the hydrogen sulphide (H2S)+CO2 (CO2) system at temperatures from 258 to 313K. *Fluid phase equilibria.* 356, 223–228. Available at: https://www.sciencedirect.com/science/article/abs/pii/S0378381213004160(Access date: 21/08/2022)

17. Chang, S and Frauke, U., 2021. Carbon Neutral China by 2060: The Role of Clean Heatin g Systems, Energies, 14, 7461. Available at: https://www.mdpi.com/1996-1073/14/22/746 1/htm (Access date: 01/07/2022)

18. Christ, C.D., Mark, A.E. & van Gunsteren, W.F., 2010. Basic Ingredients of Free Energy Calculations: A Review. *Journal of Computational Chemistry* 31, 1569–1582. Available a t: https://pubmed.ncbi.nlm.nih.gov/20033914/ [Access date: 25/08/2022].

19. De Visser, E., Hendriks, C., Barrio, M., Mølnvik, M.J., De Koeijer, G., Liljemark, S. & L e Gallo, Y., 2008. Dynamis CO2 quality recommendations. International journal of green house gas control. 2 (4), 478–484. Available at: https://www-sciencedirect-com.iclibezp1.cc.ic.ac.uk/science/article/pii/S1750583608000315 (Access date: 13/07/2022)

20. Dong, X, Gong, M, Zhang, Y, Wu, J., 2008. Vapor-liquid equilibria for 1,1,2,2-tetrafluoro ethane (R134) + fluoroethane (R161) at temperatures between (263.15 and 288.15) K, J. *Chem. Eng. Data.* Vol 53, pp 2193–2196. Available at: https://pubs.acs.org/doi/10.1021/je800505y (Access date: 14/07/2022)

21. Danesh A, Xu D-H, Todd AC., 1991. Comparative study of cubic equations of state for pr edicting phase behavior and volumetric properties of injection gas–reservoir oil systems. *Fluid Phase Equilib*, Vol 63, pp 259–78. Available at: https://www.sciencedirect.com/science/article/abs/pii/037838129180036U (Access date: 15/07/2022)

22. D.N. Theodorou, 2010. Progress and outlook in Monte Carlo simulations, *Ind. Eng. Chem. Res.* 49 (2010) 3047–3058. Available at: https://pubs.acs.org/doi/10.1021/ie9019006 (Access date: 31/08/2022)

23. Dickson, B.M., Legoll, F., Lelievre, T., Stoltz, G. & Fleurat-Lessard, P., 2010. Free energ y calculations: An efficient adaptive biasing potential method. *Journal of Physical Chemi stry* B 114, 5823–5830.Available at: https://pubs.acs.org/doi/10.1021/jp100926h[Access date: 25/08/2022].

24. D.A. McQuarrie, 1976. Statistical Mechanics, Harper and Collins, 1st edition. University Science Books, New York.

25. E. Huo, C. Liu, X. Xu, C. Dang, 2017. A ReaxFF-based molecular dynamics study of the py- rolysis mechanism of HFO-1336mzz(Z), *Int. J. Refrig*. Vol 83, pp 118–130. Available at: https://www.sciencedirect.com/science/article/abs/pii/S014070071730289X (Access d ate: 14/08/2022)

26. Frenkel, D.; Smit, B. Understanding Molecular Simulation: from Algorithms to Applicati ons, 2nd ed.; Academic Press: San Diego, CA, 2002. Available at: https://www.elsevier.com/books/understanding-molecular-simulation/frenkel/978-0-12-267351-1(Access date: 3 0/08/2022)

27. Fandiño, O., Trusler, J. & Vega-Maza, D., 2015. Phase behavior of (CO2 + H-2) a nd (CO2+ N-2) at temperatures between (218.15 and 303.15)K at pressures up to 15 MPa. Available at: https://www.sciencedirect.com/science/article/abs/pii/S1750583615000730(Access date: 26/08/2022)

28. F. G. Wang and D. P. Landau, 2001. Efficient, Multiple-Range Random Walk Algorithm to Calculate the Density of States. *Phys. Rev. Lett.* 86, 2050. Available at: https://journals.aps.org/prl/abstract/10.1103/PhysRevLett.86.2050(Access date: 09/08/2022)

29. Georg Ganzenmüllera and Philip J. Campb, 2007. Applications of Wang-Landau sampling to determine phase equilibria in complex fluids. *J. Chem. Phys.*, 127, 154504. Available at: https://aip.scitation.org/doi/pdf/10.1063/1.2794042(Access date: 09/08/2022)

30. Gong, L.-C., Ning, B.-Y., Weng, T.-C. & Ning, X.-J., 2019. Comparison of Two Efficient Methods for Calculating Partition Functions. *Entropy (Basel, Switzerland)*. 21 (11), 1050 –. Available at: https://www.mdpi.com/1099-4300/21/11/1050 [Access date: 19/08/2022].

31. Gibbs, Josiah Willard., 1902. Elementary Principles in Statistical Mechanics. New York: Charles Scribner's Sons. Available at: https://www.cambridge.org/core/books/elementary-principles-in-statistical-mechanics/E7AB3B94A215CF4E3A193C092F29856A[Access date: 05/09/2022]

32. H. Do, J.D. Hirst, R.J. Wheatley., 2011. Rapid calculation of partition functions and free energies of fluids. *J. Chem. Phys*. Vol 135, Issue 174105.

33. H. Do, J.D. Hirst, R.J. Wheatley, 2012. Calculation of partition functions and free energies of a binary mixture using the energy partitioning method: application to carbon dioxide and methane. *J. Phys. Chem*. Vol 116, Issue 4535.

34. H. Do, R.J. Wheatley, 2013. Density of states partitioning method for calculating the free energy of solids. *J. Chem. Theory Comput*. Vol 9, Issue 165.

35. H. Do, R.J. Wheatley, Reverse energy partitioning-an efficient algorithm for computing the density of states, partition functions, and free energy of solids. J. Chem. Phys. 145, 084116 (2016)

36. Hannah Ritchie, Max Roser and Pablo Rosado, 2020. *CO_2 and Greenhouse Gas Emissions*. Published online at OurWorldInData.org. [Online Resource] Available at: https://ourworldindata.org/co2-emissions(Access date: 21/08/2022)

37. Herzog, H J., 2011. Scaling up CO2 capture and storage: From megatons to gigatons, *Energy Economics*, Vol 33, pp 597-604. Available at: https://www.sciencedirect.com/science/article/pii/S0140988310001921 (Access date: 11/07/2022)

38. Intergovernmental Panel on Climate Change (IPCC), 2005. IPCC special report on CO2 capture and storage. Cambridge (United Kingdom, New York, USA): Cambridge University Press. Available at: https://www.ipcc.ch/report/carbon-dioxide-capture-and-storage/ (Access date: 04/07/2022)

39. IPCC, 2018. *Global Warming of 1.5 ℃. An IPCC Special Report on the impacts of global warming of 1.5 ℃ above pre-industrial levels and related global greenhouse gas emission pathways, in the context of strengthening the global response to the threat of climate change,,* Cambridge, UK and NY, USA: Cambridge University Press. Available at: https://www.ipcc.ch/sr15/download/ (Access date: 25/06/2022)

40. Jian-Rong Li., Yuguang Ma., M. Colin McCarthy, Julian Sculley, Jiamei Yub, Hae-Kwon Jeong, Perla B. Balbuena, and Hong-Cai Zhou., 2011. CO2 capture-related gas adsorption and separation in metal-organic frameworks. *Coordination Chemistry Reviews*. Issue 255, pp 1791-1823. Available at: https://www.sciencedirect.com/science/article/abs/pii/S0010854511000701 (Access date: 03/07/2022)

41. Kate Larsen, Hannah Pitt, Mikhail Grant, and Trevor Houser., 2021. *China's Greenhouse Gas Emissions Exceeded the Developed World for the First Time in 2019*. Rhodium Grou p. [Online Resource] Available at: https://rhg.com/research/chinas-emissions-surpass-developed-countries/(Access date: 22/08/2022)

42. Kofke DA, Cummings PT., 1997. Quantitative comparison and optimization of methods for evaluating the chemical potential by molecular simulation. *Mol Phys.* 1997;92:973–99

6. Available at: https://www.tandfonline.com/doi/abs/10.1080/002689797169600 [Acces s date: 26/08/2022]

43. Kilkis, S, Krajacic, G., Duic, N., Rosen, M.A., Al-Nimr, M.A., 2020. Advances in integra tion of energy, water, and environment systems towards climate neutrality for sustainable development. *Energy Conversion and Management*. 225, 113410. Available at: https://do i.org/10.1016/j.enconman.2020.113410 (Access date: 25/06/2022)

44. Kontogeorgis, G.M., Coutsikos, P., 2012. Thirty years with EoS/GE models—what have we learned? *Ind. Eng. Chem. Res*. 51 (11), 4119–4142. Available at: https://pubs.acs.org/d oi/10.1021/ie2015119 (Access date: 28/07/2022)

45. Kwak, T.Y., Mansoori, G.A., 1986. Van der waals mixing rules for cubic equations of stat e. Applications for supercritical fluid extraction modelling. *Chem. Eng. Sci*. 41 (5), 1303–1309. Available at: https://www.sciencedirect.com/science/article/pii/0009250986871032 (Access date: 28/07/2022)

46. Li, H., Jakobsen, J.P., Wilhelmsen, Ø. & Yan, J., 2011. PVTxy properties of CO_2 mixtures relevant for CO_2 capture, transport and storage: Review of available experimental data a nd theoretical models. *Applied energy*. 88 (11), 3567–3579. https://www.sciencedirect.co m/science/article/abs/pii/S0306261911002224 (Access date: 22/07/2022)

47. Li, J.T.; Ning, B.Y.; Zhuang, J.; Ning, X.J. 2016. Rapidly calculating the partition functio n of macroscopic systems. *Chin. Phys.* B 2016, 26, 030501. Available at: https://iopscien ce.iop.org/article/10.1088/1674-1056/26/3/030501[Access date: 19/08/2022].

48. Lachet, V., de Bruin, T., Ungerer, P., Coquelet, C., Valtz, A., Hasanov, V., Lockwood, F. & Richon, D., 2009. Thermodynamic behavior of the CO2+SO2 mixture: Experimental and Monte Carlo simulation studies. Energy Procedia. 1 (1), 1641–1647. Available at: https:// www.researchgate.net/publication/50277064_Thermodynamic_behavior_of_the_CO2SO 2_mixture_Experimental_and_Monte_Carlo_simulation_studies(Access date: 21/08/202 2)

49. Li, Y., Yu, Y., Zheng, Y. & Li, J., 2012. Vapor-liquid equilibrium properties for co nfined binary mixtures involving CO2, CH4, and N2 from Gibbs ensemble Monte Carlo simulations. *Science China. Chemistry*. 55 (9), 1825–1831. Available at: https://link.springer.com/article/10.1007/s11426-012-4724-5(Access date: 21/08/2022)

50. Liu, Z., Deng, Z., Davis, S.J. et al., 2022. Monitoring global carbon emissions in 2021. *Nat Rev Earth Environ.* Vol 3, pp 217–219. Available at: https://doi.org/10.1038/s43017-022-00285-w(Access date: 21/08/2022)

51. Li, X., Damartzis, T., Stadler, Z., Moret, S., Meier, B., Friedl, M., Marrechal, F., 2020. De carbonization in complex energy systems: a study on the feasibility of carbon neutrality f or Switzerland in 2050. *Frontiers in Energy Research*. 8, 17. [Online] Available at: https://www.frontiersin.org/articles/10.3389/fenrg.2020.549615/full (Access date: 25/06/2022)

52. Lin, J., and Zeng, J., 2021. Deciphering China's 2060 Carbon-Neutral Plan. AllianceBern stein Hong Kong Limited. [Online Resource] Available at: https://www.abfunds.com.hk/hk/en/investor/insight/deciphering-chinas-2060-carbon-neutral-plan.html(Access date: 22/08/2022).

53. Lin, B. and Xu, B., 2020. How does fossil energy abundance affect China's economic gro wth and CO2 emissions? *Science of the Total Environment,* Issue 719. Available at: https://www.sciencedirect.com/science/article/pii/S0048969720310147 (Access date: 26/06/2022)

54. Lim, Jong Sung., Park, Ji-Young., Lee, Byung-Gwon., Lee, Youn-Woo., 2002. Phase equi libria of 1,1,1-trifluoroethane (HFC-143a) + 1,1,1,2-tetrafluoroethane (HFC-134a), and + 1,1-difluoroethane (HFC-152a) at 273.15, 293.15, 303.15, and 313.15 K, *Fluid Phase Equilib*. Vol 193, pp 29–39. Available at: https://www.sciencedirect.com/science/article/abs/pii/S037838120100632X (Access date: 14/07/2022)

55. Li, H., 2008. Thermodynamic Properties of CO 2 Mixtures and Their Applications in Adv anced Power Cycles with CO 2 Capture Processes. Available at: http://kth.diva-portal.org /smash/record.jsf?pid=diva2%3A15031&dswid=4807 (Access date: 12/07/2022)

56. Li, H., Yan, J., Yan, J. & Anheden, M., 2009. Impurity impacts on the purification process in oxy-fuel combustion based CO2 capture and storage system. *Applied energy.* 86 (2), 2 02–213. Available at: https://www-sciencedirect-com.iclibezp1.cc.ic.ac.uk/science/article /pii/S0306261908001281(Access date: 12/07/2022)

57. Liu, Yu-Peng, Bo-Yuan Ning, Le-Cheng Gong, Tsu-Chien Weng, and Xi-Jing Ning., 201 9. A New Model to Predict Optimum Conditions for Growth of 2D Materials on a Substra te, Nanomaterials, 9(7), 978. Available at: https://www.mdpi.com/2079-4991/9/7/978/htm (Access date: 09/08/2022)

58. Mario Mantovani, Paolo Chiesa, Gianluca Valenti, Manuele Gatti, and Stefano Consonni, 2012. Supercritical pressure–density–temperature measurements on CO2–N2, CO2–O2 and CO2–Ar binary mixtures. *The Journal of Supercritical Fluids.* Issue 61, pp 34-43. Av ailable at: https://www.sciencedirect.com/science/article/abs/pii/S0896844611003743(Ac cess date: 06/07/2022)

59. Meng, X., Hu, X., Yang, H., and Wu, J., 2018. Vapor liquid equilibria for binary mixtures of difluoromethane (R32) + fluoroethane (R161) and fluoroethane (R161) + trans-1,3,3,3 -tetrafluoropropene (R1234ze(E)). *The Journal of Chemical Thermodynamics.* Available at: https://www.sciencedirect.com/science/article/abs/pii/S0021961417303828(Access da te: 14/07/2022)

60. Matteo C. Romano, Rahul Anantharaman, Antti Arasto, Dursun Can Ozcan, Hyungwoon g Ahn, Jan Wilco Dijkstra, Michiel Carbo, and Dulce Boavida., 2013. Application of adva nced technologies for CO2 capture from industrial sources, *Energy Procedia*, Issue 37, 71 76-7185. Available at: https://www.sciencedirect.com/science/article/pii/S187661021300 8989 (Access date: 10/07/2022)

61. M. Ramdin, T.M. Becker, S.H. Jamali, M. Wang, T.J.H. Vlugt, 2016. Computing equation of state parameters of gases from Monte Carlo simulations, *Fluid Phase Equilib*. 428, pp 174–181. Available at: https://www.sciencedirect.com/science/article/abs/pii/S0378381216302886 (Access date: 29/08/2022)

62. Mitchell, M.J.; McCammon, J.A., 1991. Free energy difference calculations by thermodynamic integration: Difficulties in obtaining a precise value. *J. Comput. Chem*. 1991, 12, 271–275. Available at: https://onlinelibrary.wiley.com/doi/abs/10.1002/jcc.540120218[Access date:29/08/2022]

63. NASA Earth Observatory, 2022. World of Change: Global temperatures. [Online] (Updated 13 Jan 2022) Available at: https://earthobservatory.nasa.gov/world-of-change/global-temperatures (Access date: 20/08/2022)

64. Nie, X., Zhao, L., Deng, S., Su, W. & Zhang, Y., 2018. A review of molecular simulation applied in vapor-liquid equilibria (VLE) estimation of thermodynamic cycles. *Journal of molecular liquids.* 264, 652–674. Available at: https://www.sciencedirect.com/science/article/abs/pii/S016773221832186X (Access date: 13/07/2022)

65. National Development and Reform Commission (NDRC), People's Republic of China, 2021. Action Plan For CO2 Peaking Before 2030. [Online], Available at: https://en.ndrc.gov.cn/policies/202110/t20211027_1301020.html (Access date: 27/06/2022)

66. Ning, B.-Y., Gong, L.-C., Weng, T.-C. & Ning, X.-J., 2021. Efficient approaches to solutions of partition function for condensed matters. *Journal of physics: Condensed matter.* 33 (11), 115901–115901. Available at: https://iopscience.iop.org/article/10.1088/1361-648X/abd33b[Access date: 19/08/2022].

67. Ning, B.Y.; Gong, L.C.; Weng, T.C.; Ning, X.J., 2019. Solution to partition function for macroscopic condensed matters—The key problem of statistical physics. arXiv, arXiv:1901.08233. Available at: https://arxiv.org/pdf/1901.08233.pdf(Access date: 09/08/2022)

68. Nicholas Metropolis, Arianna W. Rosenbluth, Marshall N. Rosenbluth, Augusta H. Teller and Edward Teller, 1953. Equation of State Calculations by Fast Computing Machines. *J. Chem. Phys.* 21, pp: 1087-1092. Available at: https://aip.scitation.org/doi/pdf/10.1063/1.1699114(Access date: 17/08/2022)

69. Peng DY, Robinson DB., 1976. A new two-constant equation of state. *Ind Eng Chem Fundam.* Vol 15, pp 59–64. Available at: https://www.researchgate.net/publication/231293953_New_Two-Constant_Equation_of_State (Access date: 20/07/2022)

70. P. Ungerer, C. Nieto-Draghi, B. Rousseau, G. Ahunbay, V. Lachet, 2007. Molecular simulation of the thermophysical properties of fluids: from understanding toward quantitative predictions, *J. Mol. Liq.* 134 (2007) 71–89. Available at: https://www.sciencedirect.com/science/article/abs/pii/S016773220600331X [Access date: 28/08/2022]

71. Redlich O, Kwong JNS., 1949. On the Thermodynamics of Solutions. V. An Equation of State. Fugacities of Gaseous Solutions. *Chem Reviews*. Vol 44, pp 233–44. Available at: https://pubs.acs.org/doi/10.1021/cr60137a013 (Access date: 20/07/2022)

72. Rackley, S.A., 2017, Carbon capture and storage. Second edition. Amsterdam, Butterworth-Heinemann. Available at: https://www.elsevier.com/books/carbon-capture-and-storage/rackley/978-0-12-812041-5 (Access date: 30/06/2022)

73. Rupal Agrawal and David A. Kofke, 1994. Thermodynamic and structural properties of model systems at solid-fluid coexistence. *Molecular Physics*. Vol 85, 1. Available at: https://www.tandfonline.com/doi/ref/10.1080/00268979500100911?scroll=top [Access date: 25/08/2022].

74. R.L. Rowley, 1994. Statistical Mechanics for Thermophysical Property Prediction, Prentice Hall. Available at: https://www.semanticscholar.org/paper/Statistical-mechanics-for-thermophysical-property-Rowley/006ce8fd55867987b0610f9a2f23bad10fca26bc (Access date: 14/08/2022)

75. Soave, G., 1972. Equilibrium constants from a modified Redlich-Kwong equation of stat e. *Chemical engineering science.* Vol 27 (6), pp 1197–1203.Available at: https://www.researchgate.net/publication/239154680_Equilibrium_Constants_From_a_Modified_Redlich-Kwong_Equation_of_State (Access date: 20/07/2022)

76. S. Lasala, P. Chiesa, R. Privat, J.-N. Jaubert, 2017. Optimizing thermodynamic models: t he relevance of molar fraction uncertainties, *J. Chem. Eng. Data*. Vol 62, pp 825–832. Av ailable at: https://pubs.acs.org/doi/10.1021/acs.jced.6b00853 (Access date: 06/08/2022)

77. S. Lasala, P. Chiesa, R. Privat, J.-N. Jaubert, 2016. VLE properties of CO2 – based binary systems containing N2, O2 and Ar: experimental measurements and modelling results wi th advanced cubic equations of state, *Fluid Phase Equilib*. Vol 428, pp 18–31. Available a t: https://www.sciencedirect.com/science/article/abs/pii/S0378381216302400 (Access dat e: 06/08/2022)

78. Tochigi, K., Kurihara, K., Kojima, K., 1995. Prediction of VLE Using Asog and Zero Pre ssure GE Mixing Rule Consistent the Second Virial Coefficient Condition. *J. Chem. Eng.* Japan 28 (5), 621–622. Available at: https://www.jstage.jst.go.jp/article/jcej/28/5/28_5_6 21/_article (Access date: 28/07/2022)

79. Taher A. Al-Sahhaf, Arthur J. Kidnay, and E. Dendy Sloan., 1983. Liquid + vapor equilibriums in the nitrogen + CO2 + methane system. *Industrial & Engineering Chemistry Fundamentals.* Vol 22, Issue 4, pp 372-380. Available at: https://pubs.ac s.org/doi/10.1021/i100012a004(Access date: 25/08/2022)

80. United Nations, 2015. *Adoption of the Paris Agreement, 21st Conference of the Parties.* P aris, United Nations. Avaliable at: https://unfccc.int/process-and-meetings/the-paris-agree ment/the-paris-agreement (Access date: 26/06/2022)

81. UNFCCC, 2019. *Climate Ambition Alliance: Nations Renew their Push to Upscale Actio n by 2020 and Achieve Net Zero CO2 Emissions by 2050. [Online]* Available at: https://u

nfccc.int/news/climate-ambition-alliance-nations-renew-their-push-to-upscale-action-by-2020-and-achieve-net-zero (Access date: 26/06/2022)

82. Valtz, C. Coquelet, A. Baba-Ahmed, D. Richon, 2002. Vapor–liquid equilibrium data for he propane+ 1,1,1,2,3,3,3-heptafluoropropane (R227ea) system at temperatures from 293. 16 to 353.18 K and pressures up to 3.4 MPa, *Fluid Phase Equilib*. Vol 202, pp 29–47. Av ailable at: https://www.sciencedirect.com/science/article/abs/pii/S0378381202000560 (A ccess date: 13/07/2022)

83. Wikipedia, 2022. Statistical mechanics. [online] Available at: https://en.wikipedia.org/wik i/Statistical_mechanics#Three_thermodynamic_ensembles [Access date: 03/09/2022]

84. W. Su, L. Zhao, S. Deng, 2017. Recent advances in modeling the vapor-liquid equilibriu m of mixed working fluids, *Fluid Phase Equilib*. Vol 432, pp 28–44. Available at: https:// www.sciencedirect.com/science/article/abs/pii/S0378381216305143 (Access date: 06/08/ 2022)

85. Wu, Z., Shi, L., Sun, R., Tian, H., Wang, X., Hu, P. & Shu, G., 2022. A temperature-indep endent prediction model predicts the vapor-liquid equilibrium of CO2-based binary mixtu res', *International Journal of Refrigeration*, 140, pp. 125-138. Available at: https://www.s ciencedirect.com/science/article/abs/pii/S0140700722001578 (Access date: 23/07/2022)

86. W.D. Cornell, P. Cieplak, C.I. Bayly, I.R. Gould, K.M. Merz, D.M. Ferguson, D.C. Spell meyer, T. Fox, J.W. Caldwell, P.A. Kollman, A second generation force field for the simul ation of proteins, nucleic acids, and organic molecules, *J. Am. Chem. Soc*. 117 (1995) 517 9–5197. Available at: https://pubs.acs.org/doi/pdf/10.1021/ja00124a002(Access date: 09/ 08/2022)

87. Xin, Z., Xiaowei, M., Boyang, C., Yuping, S., and Malin, S., 2022. Challenges toward car bon neutrality in China: Strategies and countermeasures. *Resources, Conservation and Re cycling*, Issue 176. Available at: https://www.sciencedirect.com/science/article/pii/S09213 44921005681 (Access date: 26/06/2022)

88. Yang, Wenchao., 2016. *Phase equilibrium property research of binary and multicompone nt mixture containing CO2 at low temperature*. Meng, Southeast University. Available at: https://kns.cnki.net/kcms/detail/detail.aspx?dbcode=CMFD&dbname=CMFD201701&filename=1016326794.nh&uniplatform=NZKPT&v=8JFjugiwpTGVxpWRiN0rGlh7oZNhFuIkJIRlomAmHHWHILtSBej5dAvh9mGw6wIw (Access date: 16/07/2022)

89. Yang J, Griffiths PR, Goodwin ARH., 2003. Comparison of methods for calculating ther modynamic properties of binary mixtures in the sub and super critical state: Lee–Kesler a nd cubic equations of state for binary mixtures containing either CO2 and H2S. *The Jour nal of Chemical Thermodynamics*. Vol 35, pp 1521-1539. Available at: https://www.scien cedirect.com/science/article/abs/pii/S0021961403001290 (Access date: 15/07/2022)

90. Y. Li, J. Xu, D. Li, 2010. Molecular dynamics simulation of nanoscale liquid flows, *Micr ofluid. Nanofluid*. Vol 9, pp 1011–1031. Available at: https://link.springer.com/article/10.1007/s10404-010-0612-5 (Access date: 14/08/2022)

91. Zhao, Y., Dong, X., Zhong, Q., Gong, M., Shen, J. & Wu, J. (2017) The measurements of vapor liquid phase equilibrium for R717 + R152a system at temperatures ranging from 2 53.150 K to 293.150 K. *International journal of refrigeration.* 75, 293–. Available at: http s://www.sciencedirect.com/science/article/abs/pii/S0140700716304200 (Access date: 14/ 07/2022)

92. Zhang, H., Gong, M., Li, H., Zhao, Y., Zhong, Q., Dong, X., Shen, J., Wu, J., 2016. A sim ple model for temperature-independent kij of the PR-vdW model for mixtures containing HCs, HFCs, PFCs, HFOs, CO2, RE170 and R13I1, *Fluid Phase Equilib.* 425 (2016) 374 –384. Available at: https://www.sciencedirect.com/science/article/abs/pii/S0378381216303053 (Access date: 02/08/2022)

93. Z., Shan, Y., Tao, S., Wang, H., Wang, R., Wu, L., Yun, X., Zhang, Q., Zhao, F., and Zhen g, B., 2020. Evaluating China's fossil-fuel CO2 emissions from a comprehensive dataset

of nine inventories, *Atmospheric Chemistry and Physics,* 20(19), pp. 11371-11385. Availa
ble at: https://acp.copernicus.org/articles/20/11371/2020/ (Access date: 22/07/2022)